Published for SISSA by Springer

Received: December 13, 2018
Accepted: December 15, 2018
Published: January 7, 2019

On the spectrum and string tension of U(1) lattice gauge theory in $2+1$ dimensions

Andreas Athenodorou[a] **and Michael Teper**[b]

[a] *Computation-based Science and Technology Research Center, The Cyprus Institute, 20 Kavafi Str., Nicosia 2121, Cyprus*

[b] *Rudolf Peierls Centre for Theoretical Physics, Clarendon Laboratory, University of Oxford, Parks Road, Oxford OX1 3PU, U.K.*

E-mail: a.athenodorou@cyi.ac.cy, mike.teper@physics.ox.ac.uk

Abstract: We calculate the low-lying spectra of glueballs and confining flux tubes in the U(1) lattice gauge theory in $2+1$ dimensions. We see that up to modest lattice spacing corrections, the glueball states are consistent with being multiparticle states composed of non-interacting massive $J^{PC} = 0^{--}$ particles. We observe that the $ag^2 \to 0$ limit is, as expected, unconventional, and follows the well-known saddle-point analysis of Polyakov to a good approximation. The spectrum of closed (winding) flux tubes exhibits the presence of a massive world-sheet excitation whose mass is consistent with that of the bulk screening mass. These U(1) calculations are intended to complement existing lattice calculations of the properties of SU($N \geq 2$) and SO($N \geq 3$) gauge theories in $D = 2+1$.

Keywords: Lattice Quantum Field Theory, Nonperturbative Effects, Confinement, Field Theories in Lower Dimensions

ArXiv ePrint: 1811.06280

https://doi.org/10.1007/JHEP01(2019)063

JHEP01(2019)063

Contents

JHEP01(2019)063

1 Introduction

The compact U(1) lattice gauge theory in $2+1$ dimensions is interesting because while its dynamics is non-trivial at all non-zero values of the lattice spacing a, it is to a large extent analytically tractable [1–7]. This is in contrast to both the $D = 3+1$ U(1) theory, which is essentially free on the weak coupling side of its strong-weak coupling phase transition, and also to $D = 2+1$ SU(N) gauge theories, which are (largely) analytically intractable.

While there have been many numerical studies of the 'glueball' spectrum of the U(1) theory in $2+1$ dimensions (for some recent examples see [8] or appendix E of [9] and references therein), the precision of these older calculations is inevitably quite poor compared to the precision of recent lattice studies of SU(N) [10] and of SO(N) [11] gauge theories in $D = 2+1$, and it would be useful to have something comparably precise to complement the latter. That is one of the aims of this paper. Another aim is to calculate the spectrum of non-contractible closed flux tubes that wind around one of the periodic spatial directions, so as to learn what we can about the effective world-sheet action of such flux tubes in the U(1) gauge theory, thus complementing recent studies [12, 13] of the ground state of a flux tube between static sources.

In section 2 we describe the compact U(1) lattice gauge theory and also how we calculate the masses of the particles and the energies of the winding flux tubes. We then move on, in section 3, to a summary of what one expects to find on the basis of earlier analytic work [1–7]. We give some heuristic descriptions of the screened gas of monopole-instantons and of the resulting linear confinement, and of the deconfinement transition. In section 4 we present our results for the glueball spectrum, which support the expectation that the theory is a free theory of (pseudo)scalar particles up to some lattice spacing corrections, with the mass being just the screening mass of the monopole plasma. We then calculate the flux tube spectrum, in section 5, where we find evidence for a massive mode in the world-sheet action of the flux tube. We summarise our conclusions in section 6.

2 Lattice preliminaries

2.1 Action and variables

Our U(1) variables are phases, $U_l = \exp\{i\theta_l\}$, assigned to the forward going links, l, of the lattice, and we assign $U_l^\star = \exp\{-i\theta_l\}$ when we traverse the link backwards. If the link emanates in the direction μ from the site labelled n, an alternative notation is to write U_l as $U_\mu(n)$ and similarly for θ_l. Under a local gauge transformation $V(n) = \exp\{i\phi(n)\}$ the phase on the link from the site n to the neighbouring site in the μ direction, $n+\hat{\mu}$, transforms as $U_\mu(n) \to V(n)U_\mu(n)V^\star(n+\hat{\mu})$, just like the path ordered exponential of the gauge potential along the link in the corresponding continuum gauge theory. (Although since our theory is Abelian the path ordering is not needed.) The partition function of the Euclidean lattice gauge theory is

$$Z = \int dU \exp\{-\beta S[U]\} = \prod_l \int_{-\pi}^{+\pi} d\theta_l \exp\Big\{ -\beta \sum_p (1-\cos\theta_p)\Big\}, \tag{2.1}$$

where $S[U]$ is the action of the lattice field U, and θ_p is the sum of angles on the links around the plaquette p, i.e. $\theta_p \equiv \theta_{\mu\nu}(n) = \theta_\mu(n) + \theta_\nu(n+\hat{\mu}) - \theta_\mu(n+\hat{\nu}) - \theta_\nu(n)$, if p is in the (μ,ν) plane emanating from the site n, with $\mu < \nu$. Moreover

$$\beta \overset{a\to 0}{\to} \frac{2}{ag^2}, \tag{2.2}$$

where g^2 is the gauge coupling, which in $D = 2+1$ has dimensions of mass, and so ag^2 is the dimensionless coupling on the length scale of the lattice spacing a. We work on periodic $l_x \times l_y \times l_t$ lattices.

2.2 Calculating masses and string tension

We shall give a brief and incomplete summary here. For more details, in particular of important caveats, see the discussion for the similar SU(N) calculations in [10].

Let $\mathcal{C}(x)$ be a closed and contractible space-like path on the lattice that begins and ends at the site x. Let $\Phi_{\mathcal{C}}(x)$ be the operator obtained by taking the product of the U_l phases on the links that form the boundary of $\mathcal{C}$. Since U(1) phases commute, it is obvious

JHEP01(2019)063

that $\Phi_{\mathcal{C}}(x)$ is gauge invariant. From now on we assume that we sum our operators over all the spatial sites, so that we have $p = 0$ operators at time t, which we label here $\Phi_{\mathcal{C}}(t)$. We can decompose the correlator of a generic operator Φ in terms of the energy eigenstates $|n\rangle$ and the corresponding eigenstates E_n in the standard way

$$\langle \Phi^\dagger(t)\Phi(0)\rangle = \sum_n |\langle n|\Phi|vac\rangle|^2 \exp\{-E_n t\} \stackrel{t\to\infty}{=} |\langle 0|\Phi|vac\rangle|^2 \exp\{-aE_0 n_t\}. \tag{2.3}$$

Here $|n = 0\rangle$ denotes the lightest state such that $\langle 0|\Phi|vac\rangle \neq 0$. Since in other gauge theories this ground state will normally be a single particle we will refer to it as a glueball. We have used $t = an_t$ and since n_t is our lattice variable we see that what we obtain is the value of aE_0, i.e. the energy in lattice units. By taking linear combinations of rotated operators and adding/subtracting reflections we can form operators that have a spacific spin J and parity P. Moreover the real part is $C = +$ and the imaginary part is $C = -$. So to obtain the lightest mass with specific J^{PC} quantum numbers we simply take correlators of operators with those quantum numbers. Excited states will be obtained through a variational extension of eq. (2.3) [10].

There are various important caveats including the assignment of J on a lattice, and the nature of finite volume corrections, and we refer the reader to [10] for a more complete discussion of these. Here we mention some practical considerations. Since our Monte Carlo calculation of the correlator in eq. (2.3) has statistical errors that are roughly independent of t, while the exact correlator decreases exponentially in t, it is clear that if the asymptotic exponential is to be visible we need an operator with a large enough overlap onto the ground state that this asymptotic exponential already dominates the correlator at small t. This can usually be achieved by using operators that are iteratively 'blocked' [9, 10, 14]. To evaluate the credibility of the identification of an asymptotic exponential it is useful to define an effective energy

$$C(n_t) = \frac{\langle \Phi^\dagger(n_t)\Phi(0)\rangle}{\langle \Phi^\dagger(n_t-1)\Phi(0)\rangle} = \exp\{-aE_{\rm eff}(n_t)\}. \tag{2.4}$$

If $aE_{\rm eff}(n_t)$ is consistent with being constant for $n_t \geq n_0$ then it is consistent with being described by a single asymptotic exponential for $n_t \geq n_0$ and we obtain an estimate of the energy aE_0 from the corresponding single exponential fit. Since the statistical error on $aE_{\rm eff}(n_t)$ grows exponentially in n_t such evidence for an asymptotic exponential is not necessarily convincing: one needs several consecutive values of n_t in the fit of $C(n_t)$ for which $aE_{\rm eff}(n_t)$ has small errors. This can be undermined even for small aE_0 if the overlap is small so that n_0 is large. But even if the overlap is good, but aE_0 is large, then the evidence can be weak. That is to say, our calculations of masses and energies will be most reliable for the states that are simultaneously light and have a large overlap onto our basis of operators. We shall show explicit examples later in the paper.

It is also important to note that because of the positivity properties of the expansion in eq. (2.3) we know that the exact value of $aE_{\rm eff}(n_t)$ must be monotonically decreasing with n_t. And since the typical error in identifying the effective mass plateau is to begin it at too small a value of n_t, the effect of this error is usually to overestimate the energy. So in these cases we should treat mass estimates as upper bounds on the true mass.

JHEP01(2019)063

To calculate the confining string tension we calculate the energy of a confining flux tube that winds around, say, the x direction of our finite periodic lattice. If this length is l we denote this energy by $E_f(l)$. The calculation is the same as described above for the glueballs except that the operators are built on curves $\mathcal{C}$ that are closed but non-contractible: they wind once around the x-circle. For large l we can obtain the string tension σ from the fact that $E_f(l) \to \sigma l$ as $l \to \infty$. However since $E_f(l)$ becomes large at large l, and so difficult to calculate reliably, we will in practice calculate σ from intermediate values of l where higher order corrections to the linear behaviour may be important. These higher order corrections are accurately given by the formula

$$E_f(l) = \sigma l \left(1 - \frac{\pi}{3\sigma l^2}\right)^{\frac{1}{2}} \tag{2.5}$$

which encodes all the known universal corrections [15–18] and which is known to work well in SU(N) [19–21] and SO(N) gauge theories [11] down to small values of l. We shall show below that it works equally well for U(1).

3 U(1) expectations

Naively one expects the continuum U(1) theory to be a free field theory of massless photons. That is to say, if one takes the limit $\beta = 2/ag^2 \to \infty$ and expresses quantities in units of g^2 then what one obtains is a free theory of massless particles. Of course if one places charged static sources a distance r apart into the theory then one obtains a non-trivial Coulomb potential which is logarithmically confining, $V(r) = \{g^2/\pi\} \log r$ in $D = 2+1$. If the theory were non-Abelian, then perturbation theory would produce an additional series of higher order corrections in increasing powers of $g^2 r$ (the dimensionless coupling on the scale r) but this of course could only be trusted when $g^2 r$ is small. In fact for large r we know that in any gauge theory the potential $V(r)$ cannot grow faster than $\propto r$ [22]. (Heuristically, in a confining flux tube a faster growth would imply a diverging energy density and hence a breakdown of the vacuum.) In our Abelian U(1) case perturbation theory simplifies and we only have the logarithmic Coulomb piece up to lattice spacing corrections, although this may cease to hold in a finite volume [23]. Of course, as we shall summarise below, in the U(1) lattice gauge theory the vacuum contains a dilute gas of instantons which drive the screening of the U(1) fields, so that the perturbative contributions will be exponentially suppressed at large enough r for any non-zero lattice spacing.

As remarked above, at finite a the compact U(1) lattice gauge theory possesses non-trivial physics which is driven by the instantons of the theory [1–4]. In Euclidean $D = 2+1$ the field of this instanton is just like the field of a magnetic monopole in 3 space dimensions. So we shall follow convention and refer to the instantons as monopoles or monopole-instantons, and we shall often refer to their fields as 'magnetic', although these fields point out in both timelike and spacelike directions. These are singular Dirac monopoles with a diverging ultraviolet action and this makes possible reliable saddle-point calculations [1–3]. One finds that the magnetic fields are screened with a screening mass m_D that sets the screening length [1–3]. This is the mass gap, the lightest particle in the theory, and it

JHEP01(2019)063

possesses $J^{PC} = 0^{--}$ quantum numbers. Thus the vacuum contains a screened plasma of monopole-instantons and, in addition, one can show that this generates a linearly confining potential betwen static charged sources, with a string tension σ. One finds, using $\beta = 2/ag^2$, [1–3, 5–7]

$$a^2 m_D^2 \stackrel{\beta\to\infty}{=} c\beta \exp\{-\tilde{c}\beta\} \tag{3.1}$$

and

$$a^2\sigma \stackrel{\beta\to\infty}{=} c' a g^2 a m_D. \tag{3.2}$$

Here the (semi)classical values of the various constants are

$$\tilde{c} = 0.2527\pi^2, \qquad c = \sqrt{8\pi^2}, \qquad c' = \frac{8}{\sqrt{2\pi^2}} \tag{3.3}$$

where $\tilde{c}$ is directly related to the action of an isolated monopole on the lattice. We see that both m_D/g^2 and $\sqrt{\sigma}/g^2$ vanish as $\beta = 2/ag^2 \to \infty$. Thus we have a trivial massless free field theory if we take the continuum limit keeping g^2 as our fixed scale. However since g^2 is not directly physical one might instead choose to take the continuum limit keeping m_D fixed. In this case we see from the above that $\sigma/m_D^2 \to \infty$ as $a \to 0$, so any putative glueballs formed of closed loops of flux will become infinitely massive and will decouple from the theory. Thus we are left with a theory of free massive scalar particles in this way of defining the continuum limit. The above are heuristic arguments, but can be made much more precise by saddle point calculations [1–3] and the main conclusions can be made rigorous [5–7].

Because the monopoles play a fundamental role in the physics of the U(1) theory we describe them in more detail in section 3.1 and explain why we have screening. (For a more extensive and pedagogical analysis see for example [23–25].) At the qualitative level it is very simple to see how such monopoles produce linear confinement, and we provide the argument in section 3.2. We then discuss the deconfining transition at finite temperature, together with some numerical illustrations, in section 3.3. Finally we make some observations on the consequences of taking different scales to define our continuum limit. It is the fact that the monopoles are ultraviolet objects that makes possible simple heuristic arguments that capture the essential dynamics. At the same time the fact that monopoles consist of near-maximal field fluctuations on the scale of a means that our computer simulations inevitably encounter a severe form of critical slowing down which limits how far in β we can easily go.

3.1 Monopoles (instantons) and screening

To motivate how one identifies the presence of a monopole-instanton in a U(1) lattice gauge field it is useful to think of the lattice field as being embedded in a continuous U(1) gauge field. It will be convenient, because the $D = 2+1$ space-time is Euclidean, to use a notation that is appropriate to 3 space dimensions. For example, our 'magnetic' flux will not be the (pseudo)scalar of 2 space dimensions but rather the vector of 3 space dimensions.

We recall that the variable on each link l is the phase $\exp\{i\theta_l\} \equiv \exp\{i\theta_\mu(n)\}$ where l is the link emanating in the positive μ direction from the lattice site n and $\theta_l \in (-\pi, +\pi]$.

JHEP01(2019)063

In the continuum limit, with fields smooth on the scale of a, $\theta_\mu(n)$ becomes simply the gauge potential in lattice units. To be more precise, given how $\exp\{i\theta_l\}$ transforms under a gauge transformation, it corresponds to the exponential of the integral of gauge potential along the link l, i.e.

$$\theta_\mu(x) \sim \int_x^{x+a\hat{\mu}} ds A_\mu(s). \tag{3.4}$$

So if we sum the angles on the link matrices around a plaquette p (conjugated when they are backward going) then we obtain the total magnetic flux B_p through any surface which is bounded by that plaquette's boundary and on which the fields are not singular

$$\theta_p = \sum_{l\in\partial p} \theta_l = \int_{\partial p} ds A_l(s) = B_p, \tag{3.5}$$

where A_l is the component along the link l. Note that the flux has a direction and reverses sign if we reverse the order in which we go around the plaquette. (Clearly $\theta_l \to -\theta_l$ under this operation.) Consider then a lattice cube c. It is clear that the sum of the angles around the bounding plaquettes of c must be zero because for each link matrix on a plaquette there is also its conjugate from a neighbouring plaquette, i.e.

$$\sum_{p\in\partial c} \theta_p = 0. \tag{3.6}$$

Indeed this is true for any closed surface, not just a cube. Thus if there is no singularity of the gauge potential on any of the plaquettes then

$$\sum_{p\in\partial c} B_p = 0, \tag{3.7}$$

i.e the net flux out of the cube is zero and we have no magnetically charged object within the cube. (Here p is an oriented plaquette so that B_p is a flux emanating out from the centre of the cube.) Now suppose we have large fluctuations on the plaquettes around a cube. In particular let us suppose the angles sum to $\pi/3$ on each of 5 of the 6 plaquettes. Then by eq. (3.6) we know that on the 6'th plaquette we have $B_p = -5\pi/3 = \pi/3 - 2\pi$ if there are no singularities on this plaquette. So now the question we must ask is, do we in fact have a singularity on this plaquette? If we have a minimal singularity then encircling the singularity provides the -2π. and the actual flux will be just $\pi/3$. That is to say, we have a minimally charges Dirac monopole within the cube with a Dirac string piercing the 6'th plaquette. Since the energy (action) density is $\propto B^2$, it is clearly much more likely that there is a Dirac string piercing the sixth plaquette, and hence a magnetic flux $\pi/3$, rather than no string and hence the much larger magnetic flux of $-5\pi/3$ through the plaquette. This simple argument essentially transposes to the lattice the elegant argument by Dirac in the continuum theory [26]. This way of identifying monopoles is the standard lattice algorithm [27]: one decomposes each sum of plaquette angles into

$$\theta_p = 2\pi n_p + \tilde{\theta}_p\,; \qquad \tilde{\theta}_p \in (-\pi, +\pi) \tag{3.8}$$

JHEP01(2019)063

and the monopole charge in the cube is then the sum of the integers n_p on the oriented plaquettes bounding the cube. If we now consider such a monopole on the lattice then the same argument can be applied to any larger surface enclosing the monopole. If we have a monopole that is a long way from other (anti-)monopoles then a small smooth deformation of the fields cannot remove it (although it may move it to a neighbouring cube). Thus an isolated monopole in an infinite volume is at a minimum of the action (which may in general include zero-modes). That is to say these are instantons which can form the basis for a saddle-point calculation. Since a monopole's presence in a cube is tied to a Dirac string leaving the cube through one of its faces (or a net number of Dirac strings leaving the cube) and since each face is shared with a neighbouring cube, it is clear that in a finite periodic volume a monopole must be partnered by an anti-monopole so that the net magnetic charge is zero and the net magnetic flux out of the space-time volume is also zero.

We should mention that much of the analytic work has been performed using the Villain lattice action [28] which is in the same universality class as our plaquette action. In addition to the angles on the links it contains explicit integer valued variables living on the plaquettes which when summed over the faces of a cube can be shown to provide a direct definition of the monopole charge within that cube. It is natural to ask how closely these monopoles are related to those that are extracted using eq. (3.8). The numerical answer is that outside the region near $\beta \sim 0$ of very strong coupling, the monopole gases obtained by these two definitions differ almost always by no more than a number of small dipoles which have no impact on the long distance physics of the theory [29].

Since the monopoles are pointlike and have an action that is ultraviolet large, they would appear to be ideal candidates for being treated as a dilute gas of instantons. However if we consider such a dilute gas then we immediately see a problem: the interaction energy/action of the monopole with the dilute gas diverges. This is because the potential energy with a single (anti-)monopole $\propto \pm 1/r$. Within a shell a distance r from the monopole we have a number of monopoles and anti-monopoles that is proportional to the volume of the shell, i.e. $n_M(r), n_{\bar{M}}(r) \propto r^2$. This is a dilute gas so the modulus of the net magnetic charge is $|n_M(r) - n_{\bar{M}}(r)| \propto \sqrt{r^2} \sim R$ and the contribution to our original monopole's energy is $\propto \pm r \times 1/r \sim \pm r^0$. Integrate this over r with random signs and one has a divergence. To control these divergences the gas needs to have some order rather than being completely random: this will obvously decrease the entropy but may render the energy well defined. The answer is well known from the physics of a plasma of charged particles in three spatial dimensions: the particles of the gas order themselves in such a way as to induce screening. At large distances the field of our monopole is screened so that its field falls exponentially with r and the interaction energy is finite. The inverse screening length defines a screening mass, m_D, which more careful calculations show to be given by eq. (3.1). This is essentially a screened photon and has $J^{PC} = 0^{--}$ quantum numbers.

3.2 Monopoles and confinement

Once we know that the monopoles organise themselves into a screened gas it is straightforward to predict the qualitative impact on the potential $V(r)$ between static charges a distance r apart. Consider a rectangular Wilson loop of extent $r \times \tau$ in the spatial and

JHEP01(2019)063

temporal directions respectively. Then, as is well known, if we integrate the gauge potential around the Wilson loop and exponentiate it and take the expectation value and take $\tau \to \infty$, we will obtain the potential between the two static charges. This is true for general gauge theories and here we can write it as

$$\left\langle \exp\left\{ i \int_{r\times\tau} A ds \right\} \right\rangle = \langle \exp\{iB(r,\tau)\}\rangle \overset{r,\tau\to\infty}{=} c(r) \exp\{-V(r)\tau\}, \tag{3.9}$$

where we use the fact that integrating the potential around the loop gives us the magnetic flux passing through the rectangular surface spanned by the loop, up to an additive integer multiple of 2π coming from Dirac strings which clearly does not affect the value of $\exp\{iB(r,\tau)\}$.

To calculate the contribution of the monopole gas to $B(r,\tau)$ we make the (inessential) approximation that the flux of any monopole within a slab extending a distance of $l_D = 1/m_D$ either side of the Wilson loop is not screened at all and the gas therein is random, while monopoles further away are completely screened. Thus $B(r,\tau)$ only receives contributions from monopoles within the space-time slab. Assuming a symmetric flux from each monopole and given that r and τ are arbitrarily large, half of the flux, i.e. π units, will pass through the rectangle. (We neglect the vanishing fraction of monopoles near the boundary.) Given that this is a random dilute gas, we can use the Poisson distribution for the probability of having a particular number of (anti)monopoles. In this approximation we can factorise the contributions of monopoles and antimonopoles, and those from the lower and upper slabs since the magnetic flux is additive. Moreover the contribution of any (anti-)monopole to $B(r,\tau)$ is $\pm\pi$ and when exponentiated in eq. (3.9) this just gives a factor of $\exp\{\pm i\pi\} = -1$. We can place each monopole anywhere in the volume $l_D r\tau$ of the slab, and the probability of finding one in a unit volume is $c(\beta) \propto \exp\{-\beta S_M\}$ where S_M is the action on the lattice of an isolated monopole. Thus we have the estimate

$$\langle \exp\{iB(r,\tau)\}\rangle = \left(\sum_n \frac{(c(\beta) l_D r\tau)^n}{n!} e^{-\bar{n}} (-1)^n \right)^4 = e^{-8\bar{n}} = e^{-8c(\beta) l_D r\tau}, \tag{3.10}$$

where the average number of monopoles is $\bar{n} = c(\beta) l_D r\tau$ in such a Poisson distribution, and the power of 4 comes from multiplying the contribution of the slabs on both sides and doing all this for monopoles and antimonopoles separately. Comparing to eq. (3.9) we see that the monopoles produce a linearly confining potential between the charges

$$V(r) = 8c(\beta) l_D r = \frac{8c(\beta)}{m_D} r = \sigma r \tag{3.11}$$

with a string tension σ. Given the various approximations we made in this argument, we should not expect our expression for σ to match the exact expression for σ in eq. (3.2). However since $c(\beta)$ in eq. (3.11) is proportional to $\exp\{-\tilde{c}\beta\} \propto m_D^2$ in eq. (3.1), we see that in eq. (3.11) we have $\sigma \propto m_D$ just as in eq. (3.2). In any case the approximations do not affect the qualitative argument and the above calculation captures the reason why a screened monopole gas produces a linearly confining potential between static charges.

JHEP01(2019)063

3.3 Deconfinement

As we have seen above the monopole-instantons in the U(1) lattice gauge theory in an infinite Euclidean space-time volume generate linear confinement. This corresponds to a temperature $T = 0$. At some finite $T = T_c$ we can expect the theory to deconfine. If the correlation length diverges at T_c then one expects [30] the transition to be in the same universality class as the spin model in one lower dimension that encodes the centre symmetry of the gauge theory. Here the centre is U(1) and we are in $D = 2 + 1$, so the spin model is the XY model in $D = 2$. So the relevant phase transition is the Kosterlitz-Thouless transition which is of infinite order [31]. Such a transition is challenging to study numerically although some lattice studies of the the U(1) transition and its critical exponents do exist [32–34]. We do not intend to study the transition in this paper but we do need to know enough about it to be confident that our calculations in this paper are indeed in the low-T confining phase. We will begin by showing how we expect T_c to scale and then we will display some typical numerical signals of the transition.

We start with a well-known general argument and then proceed to a more specific dynamical argument. Consider a flux tube attached to sources a large distance l apart at temperature T. The contribution to the partition function $Z(T)$ is

$$\delta Z(T) \sim N(l) \exp\left\{-\frac{E(l)}{T}\right\}, \tag{3.12}$$

where $N(l)$ is the number of flux tubes between the sources, i.e. the 'entropy' factor, and $E(l)$ is the energy of the flux tube. (In this heuristic argument we make the simplifying approximation that the flux tubes are all of length l.) For large l we have $E(l) \simeq \sigma l$ where σ is the string tension, and one can easily show that the dominant behaviour of $N(l)$ is exponential in l with the scale set by the flux tube width l_0 i.e.

$$\delta Z(T) \propto \exp\left\{\frac{cl}{l_0}\right\} \exp\left\{-\frac{\sigma l}{T}\right\} = \exp\left\{\left(\frac{c}{l_0} - \frac{\sigma}{T}\right) l\right\}, \tag{3.13}$$

where the dimensionless constant $c = O(1)$ depends on details, and we ignore sub-leading power factors in $N(l)$ since they do not affect the argument. It is clear from eq. (3.13) that as we increase T at some value $T = Tc$ the entropy factor will overwhelm the energy factor and $\delta Z(T)$ will diverge as $l \to \infty$. So for $T > Tc$ the vacuum contains a condensate of arbitrarily long flux tubes and so it costs nothing to increase l, i.e. the theory is deconfining. From eq. (3.13) we see that this occurs at

$$T = T_c = \frac{\sigma l_0}{c} = \frac{\tilde{c}\sigma}{c m_D}, \tag{3.14}$$

where we assume that the width of the flux tube is $l_o = \tilde{c}/m_D$ with $\tilde{c} = O(1)$ since the screening mass, m_D, is the fundamental dimensionful dynamical quantity in the theory. Now from eqs. (3.1), (3.2) we see that this means that

$$aT_c \propto 1/\beta \Longrightarrow \frac{T_c}{g^2} \stackrel{a\to 0}{=} \text{constant}. \tag{3.15}$$

JHEP01(2019)063

This is interesting and somewhat counterintuitive: whereas the other nontrivial dynamical quantities such as m_D and σ have the unusual behaviour $\propto \exp\{-c/ag^2\}$ as $a \to 0$ (arising from the ultraviolet nature of the instanton dynamics) the deconfining temperature has a conventional scaling continuum limit.

We now complement the above general argument with a derivation of T_c that relies more closely on the U(1) dynamics, and which will therefore allow us to obtain more details of the transition. We saw earlier that linear confinement can be attributed to the flux from the monopole-instantons that are within a screening length $l_s = 1/am_D$ of the Wilson loop. The calculations rely on a symmetric radial flux from the monopoles but this is only exactly true in a Euclidean space-time volume that is infinite in all directions, and hence is at $T = 0$. For $T > 0$ the timelike extent is $L_t = 1/T$. Since the boundary is periodic the magnetic flux cannot pass through it and will be directed in a purely spatial direction once it is far enough from the monopole. So if we are a distance $r \gg 1/T$ from the monopole the 2π of flux will be equally distributed over a cylindrical surface of area $A = 2\pi r L_t = 2\pi r/T$ so that the flux density is $B = 2\pi/A = T/r$. To obtain the total action $E_M(R)$ of the monopole field within a distance $R \gg 1/T$ we integrate the action density B^2 over the radius r, the angle θ and Euclidean time τ to obtain, approximately,

$$E_M(R) \propto \int_0^{1/T} d\tau \int_a^R r dr \int_0^{2\pi} d\theta B^2(r) \propto 2\pi T \log R. \tag{3.16}$$

So as the spatial volume increases to infinity, the action of a monopole diverges logarithmically with the spatial size. This is of course precisely the behaviour of vortices in the $D = 2$ XY model. This is no surprise: for $R \gg L_t = 1/T$ the monopole fields are in a thin slab pointing radially outwards and thus directly mimicking a $D = 2$ vortex with radially pointing spins. And the argument for a phase transition is the same as in the XY model. Consider a monopole in a space-time volume $R^2 L_t$. Its contribution to the partition function will be

$$\begin{aligned} \delta Z(R,T) \propto R^2 L_t \exp\{-\beta E_M(R)\} &\propto \exp\{2\log R\} \exp\{-2\pi\beta T \log R\} \\ &\propto \exp\{2(1-\pi T\beta)\log R\} \end{aligned} \tag{3.17}$$

since the monopole can be placed anywhere in the volume $R^2 L_t$ (its entropy) and we have used eq. (3.16) and $L_t = 1/T$ (and we drop factors that can be neglected). We see that because the divergence of the action with R is only logarithmic it can be overcome by the trivial entropy factor that arises from translating the position of the monopole; so as $R \to \infty$ the weight of the monopole vanishes for $T > 1/\pi\beta$ and diverges for $T < 1/\pi\beta$, indicating a phase transition at $T = T_c = 1/\pi\beta$. All this can be trivially extended to a dilute gas of monopoles and so we expect a phase transition at

$$T_c = \frac{c}{\beta} \tag{3.18}$$

for some constant c which is just $1/\pi$ in the simple calculation above. For $T < T_c$ we have a gas (condensate) of monopoles which will produce a linearly confining force between charges, while for $T > T_c$ the entropy no longer wins out over the action and any monopole

cannot exist in isolation but must be bound to a neighbouring (anti-)monopole in a dipole, i.e. the monopoles are 'confined' and the argument for the linear confinement of charges breaks down.

All this strongly suggests that the transition should be in the same universality class as that of the XY model, i.e. of infinite order. Some earlier lattice calculations have attempted to calculate the critical exponents of this transition and these appear to be consistent with that expectation [32–34]. We note that the above argument only works if $L_t = 1/T < 1/m_D$ where m_D is the screening mass. If $L_t > 1/m_D$, so that the monopole fields are screened away before they reach the time boundary, then the monopole will not be affected by the temporal periodicity. However, since $1/T_c \propto \beta$ while $1/m_D \propto \exp\{+c\beta\}$, we will always satisfy $1/T < 1/m_D$ when T is near T_c as long as β is not too small.

Although we do not intend to study deconfinement in this paper — all our calculations are intended to be in the $T \sim 0$ confined phase — we wish to reassure ourselves that our values of L_t do indeed satisfy $T = 1/L_t \ll T_c$. We have therefore performed calculations on $L^2 L_t$ lattices with $L_t = 8$ and $L = 32, 64, 96$ to identify the approximate location in β of the deconfining transition. We do this in the conventional way by first taking the Polyakov loop, which is defined as the product of link variables along a circle that winds once around the temporal circle. Call it $l(x, y)$ where (x, y) is the spatial position in the time-slice where we start the loop. We then average $l(x, y)$ over x, y and take the modulus of this average, before averaging over all fields: i.e. we use as our 'order parameter' for the transition

$$\langle |\bar{l}| \rangle = \langle | \frac{1}{N_s} \sum_{x,y} l(x, y) | \rangle, \tag{3.19}$$

where N_s is the number of lattice sites in a time-slice. The reason for this somewhat ugly modification of the Polyakov loop expectation value is the same as in SU(N) gauge theories: for $T > T_c$ the centre symmetry is spontaneously broken in an infinite volume, but in a finite volume (such as ours) the system will tunnel through to the various vacua so that in a sufficiently long calculation we will find $\langle l \rangle = 0$ for all T. On the other hand $\langle |\bar{l}| \rangle$ will be the same in all these vacua (the typical lattice field will be in one vacuum) so it suffers no cancellations and should be 'large' in the deconfined phase. This is at a price: $\langle |\bar{l}| \rangle$ will also be non-zero in the confined phase, but this value will be small and will vanish as $L \to \infty$. So while this variable is a little ugly theoretically, it can serve the purpose of identifying the crossover between phases on a finite volume. So we plot $\langle |\bar{l}| \rangle$ on our $L^2 8$ lattices in figure 1. For clarity we have renormalised the data for the different L so that they have the same value at $\beta = 2.0$, which clearly lies away from the transition region. We see a very clear cross-over from small to large values with the steepest rate of change somewhere around $\beta_c \sim 2.5$, although β_c increases slightly with increasing L, something which would have been more apparent if we had not renormalised the data. If we had not renormalised then we would have seen that $\langle |\bar{l}| \rangle$ decreases with increasing L. So this has the characteristics of the expected deconfining transition. It is useful and conventional to complement this analysis with the susceptibility of the same quantity. This we display in figure 2 for our three spatial volumes: $L = 64$. This confirms that the transition lies in the region $\beta_c \sim 2.5$. These calculations are not an attempt to add to earlier work [32–34] but

JHEP01(2019)063

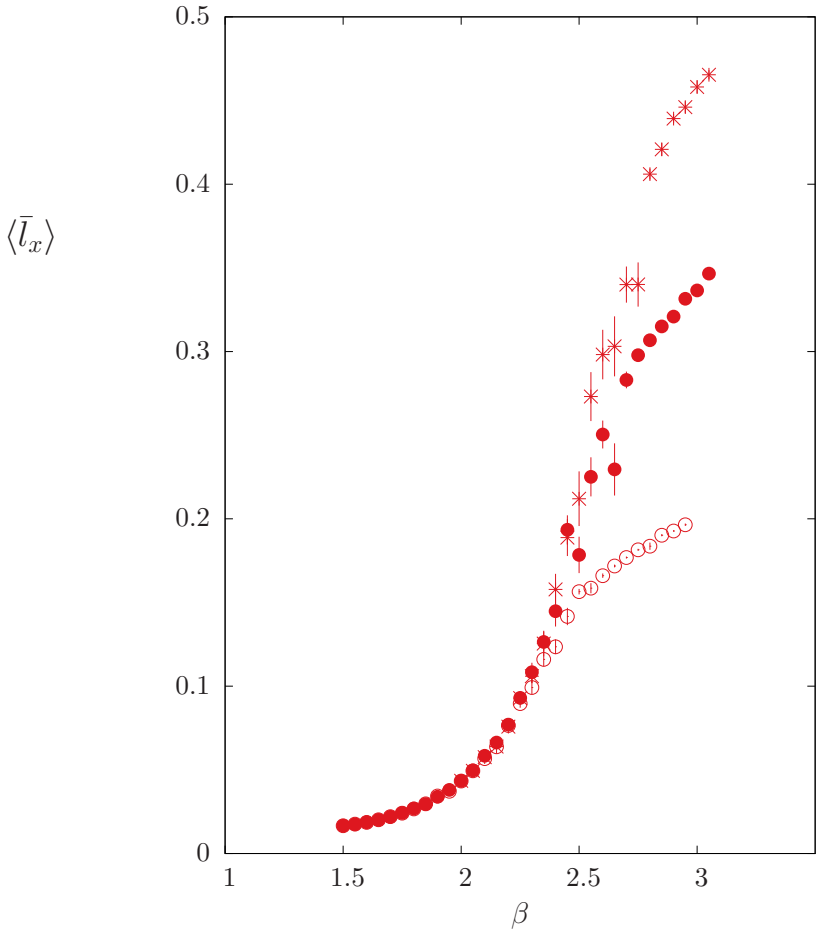

Figure 1. Values of $\langle \bar{l}_x \rangle$ on $8 \times 96 \times 96$, $\star$, $8 \times 64 \times 64$, $\bullet$, and $8 \times 32 \times 32$, $\circ$, lattices, rescaled to common values at smallest β.

simply to tell us how large a lattice we need to use to be well within the confining phase in our range of β. Given that $L_t^c = 1/T_c \propto \beta$ to leading order, we infer that we will need our lattices to have $L, L_t \gg 8\beta/2.5$ to satisfy this requirement.

We remarked that T_c/g^2 is non-zero as $\beta \to \infty$. However as is apparent from the above, all the physical differences between the two phases will disappear $\propto \exp\{-c\beta\}$ as $\beta \to \infty$, so despite its conventional scaling, the phase transition will effectively disappear if we approach the continuum limit in the conventional fashion by taking g^2 as our physical scale. If on the other hand we take m_D as our physical scale, then in this continuum limit $T_c/m_D \to \infty$ and the deconfinement transition disappears from the theory.

3.4 Continuum limit(s)

As we remarked above, a formal treatment of the U(1) theory tells us that the continuum theory is a free field theory of massive particles which, moreover, is linearly confining at any non-zero lattice spacing [5–7]. In the U(1) lattice theory there are several possible length scales that one might consider keeping fixed as one approaches the continuum limit, $a \to 0$.

JHEP01(2019)063

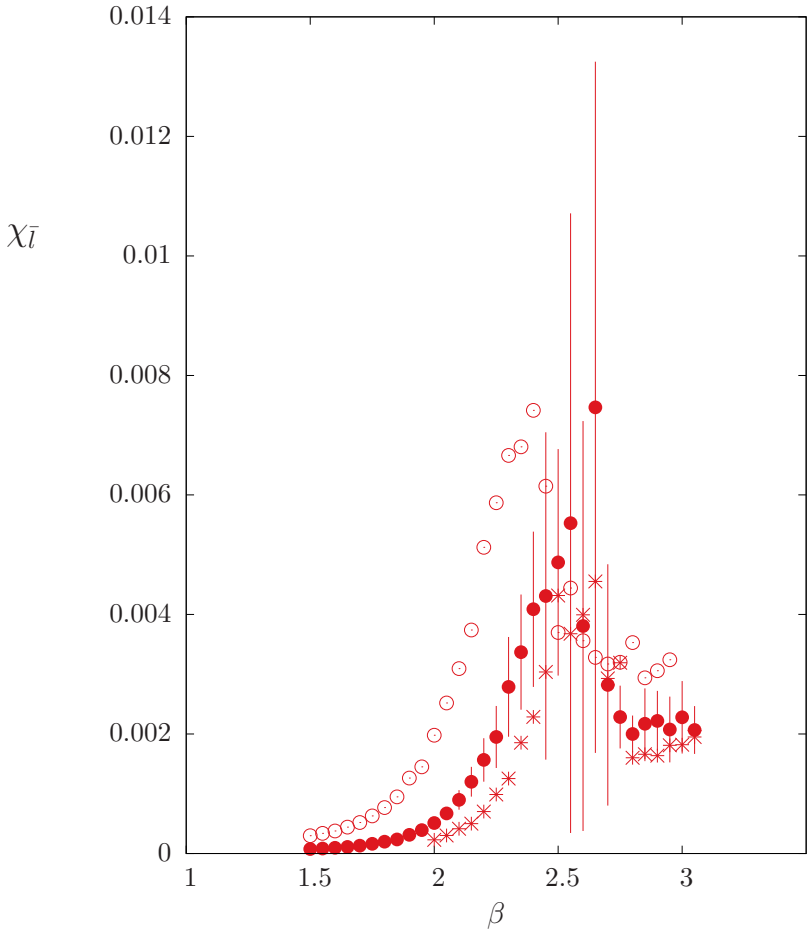

Figure 2. The (vacuum-subtracted) susceptibility of $|\bar{l}_x|$ on 8×32^2 ($\circ$), 8×64^2 ($\bullet$) and 8×96^2 ($\star$) lattices. For clarity only errors on the $l = 64$ points are shown.

These are the inverse coupling, $l_g = 1/g^2$, the inverse string tension, $l_\sigma = 1/\sqrt{\sigma}$, the inverse screening mass, $l_D = 1/m_D$, and the average separation between the monopole-instantons, l_M. Expressions relating the first three length scales are given in eqs. (3.1), (3.2), so we see that $l_D \sim g^2 l_\sigma^2$. The scale l_M gives us the average number of monopoles in a space-time volume $\bar{n}(V) = V/l_M^3$. So from eq. (3.11) we deduce that

$$l_M^3 \sim l_\sigma^2 l_D. \tag{3.20}$$

It is interesting to see what kind of 'continuum limit' one might obtain in keeping each of these length scales fixed. In asking this question we need to express our lengths and energies in units of the fixed physical length and energy scale (with the latter being the inverse of the former).

(1) l_g *fixed as* $a \to 0$. In this limit the average separation between the monopole-instantons grows $\propto \exp\{+c/ag^2\}$ where $c > 0$ so on any fixed length scale r such that $r/l_g < \infty$, there are no monopoles at all in the $a \to 0$ continuum limit and

JHEP01(2019)063

there is no linear confinement. That is to say if we introduce charged sources a distance r apart such that $r/l_g < \infty$ then the potential energy is simply the logarithmic Coulomb one. We also have $m_D = 0$ in this limit so that the theory is a free field theory of massless 'photons'. Of course in this free continuum field theory the coupling g^2 does not provide a scale, since it can be absorbed into the fields, whereas in the lattice theory it cannot be simply absorbed away because the fields are integrated over a compact range so the coupling would reappear in the range of integration.

(2) l_σ *fixed as* $a \to 0$. In this limit physical distances are some finite multiple of l_σ and physical energies are some finite multiple of $E_\sigma = 1/l_\sigma = \sqrt{\sigma}$. From eq. (3.2) we see that

$$\frac{m_D}{E_\sigma} = \frac{\sqrt{\sigma}}{g^2} \stackrel{\beta\to\infty}{\longrightarrow} 0, \tag{3.21}$$

i.e. we have a theory of massless particles. If we insert charged sources then we can consider separately the linear potential, $V_\sigma = \sigma r$, and the Coulomb potential, $V_c \sim g^2 \log r$. If we change the distance from $r_1 = \hat{r}_1 l_\sigma$ to $r_2 = \hat{r}_2 l_\sigma$ the change in the linear potential in physical units is $\delta V_\sigma / E_\sigma = (\hat{r}_2 - \hat{r}_1)$ which is finite. However this is deceptive: the linear potential can only appear on scales $r \gg 1/m_D$ and since $m_D/E_\sigma \stackrel{\beta\to\infty}{=} 0$ we have in fact no linear potential at any finite physical distance in this continuum limit. (Although it will be there at finite β at large enough r.) What we have at finite r is just the Coulomb potential, which is not screened since $m_D = 0$ in this continuum limit. The change in that potential in going from $r_1 = \hat{r}_1 l_\sigma$ to $r_2 = \hat{r}_2 l_\sigma$ is, in physical units,

$$\frac{\delta V_c}{E_\sigma} = \frac{g^2 \log\{\hat{r}_2/\hat{r}_1\}}{\pi\sqrt{\sigma}} \stackrel{\beta\to\infty}{\longrightarrow} \infty. \tag{3.22}$$

Thus we cannot couple charged particles to the theory in this limit.

(3) l_D *fixed as* $a \to 0$. In this case the screening mass in physical units is finite by definition since $m_D/E_D = 1$ where $E_D = 1/l_D = m_D$. So the theory is one of massive particles. If we now couple charged sources a distance $r = \hat{r} l_D$ apart then we will have a linear potential $V_\sigma \simeq \sigma r$ as long as $r \gg l_D$, and a Coulomb potential for $r \ll l_D$, which becomes screened at larger r. The change in the linear potential when we increase r from r_1 to r_2 is

$$\frac{\delta V_\sigma}{E_D} = \frac{\sigma(\hat{r}_2 l_D - \hat{r}_1 l_D)}{E_D} = \frac{\sigma(\hat{r}_2 - \hat{r}_1)}{m_D^2} = \frac{g^2}{m_D}(\hat{r}_2 - \hat{r}_1) \stackrel{\beta\to\infty}{\longrightarrow} \infty, \tag{3.23}$$

where we have used eq. (3.2). A similar argument shows that the change in the Coulomb potential is $\delta V_c/E_D = (g^2/\pi m_D)\log\{\hat{r}_2/\hat{r}_1\}$ which also diverges as $\beta \to \infty$. So in this case as well we cannot couple charged particles to the theory.

(4) l_M *fixed as* $a \to 0$. If we use l_M as our fixed unit of length then, by definition, our fields will contain a finite non-zero density of monopoles. The corresponding energy scale is $E_M = 1/l_M$ and one can easily see, using eqs. (3.20), (3.1), (3.2), that

$$\frac{m_D}{E_M} = \{g^2 l_D\}^{-\frac{1}{3}} \stackrel{\beta\to\infty}{\longrightarrow} 0 \tag{3.24}$$

JHEP01(2019)063

so this continuum limit has massless particles. If we now consider the linear confining potential $\sim \sigma r$ between two sources a distance r apart, and if we ask by how much this potential changes between $r_1 = \hat{r}_1 l_M$ and $r_2 = \hat{r}_2 l_M$ then we find that this change, in units of our energy scale E_M is divergent:

$$\frac{\delta V_\sigma}{E_M} = \frac{\sigma(\hat{r}_1 - \hat{r}_2) l_M}{E_M} = \frac{l_M^2}{l_\sigma^2}(\hat{r}_1 - \hat{r}_2) \propto \{g l_M\}^{\frac{1}{2}} \overset{\beta\to\infty}{\to} \infty. \tag{3.25}$$

Similar manipulations show that the same is true for the Coulomb potential. All this means that we cannot add charged sources (or particles) to the theory if this is to constitute a sensible continuum limit.

What we infer from the above is that in none of these candidate continuum limits do we see a linearly confining potential. In some the string tension diverges in physical units, while in others the transition from Coulomb to linear only occurs at infinite separation. (Of course on the lattice at finite β there are no divergences.) A corollary is that in none of these limits do we have non-perturbative glueballs composed of contractible closed loops of flux. Either such states are ultraviolet, or the 'flux tube' width, $\sim 1/m_D$, is infinite. So the only particle is the screened 'photon'.

4 Glueballs and string tension

As remarked above, the expectation is that in the continuum limit we have a free theory of massive scalar particles. So when we calculate the mass spectrum we expect the lightest particle to be a 'massive photon' in the $J^{PC} = 0^{--}$ sector with the mass m_D given in eq. (3.1). All other states will be states composed of two or more of these particles which will be free up to finite lattice spacing corrections. Thus we expect the lightest 0^{++} state to consist of two of these photons with zero relative momentum, and the first excited 0^{--} state to consist of three of these photons with zero relative momentum, i.e.

$$m^{gs}_{0^{--}} = m_D\,; \qquad m^{gs}_{0^{++}} = 2m_D\,; \qquad m^{ex1}_{0^{--}} = 3m_D. \tag{4.1}$$

Other states will have photons with momenta that are non-zero, and these need not be free momenta due to phase shifts induced by interactions due to lattice spacing corrections. Moreover they will typically have small gaps with other excitations (on a large volume) so their analysis is more complicated and goes beyond the scope of this paper. So we shall focus on the ground and first excited 0^{--} states and the ground 0^{++} state, and see whether we can confirm the expectation in eq. (4.1), and also that in eq. (3.1), at least as far as the functional dependence on β is concerned.

The tension of the confining string is the other quantity we calculate in this section. While one is used to continuum limits in which dimensionless mass ratios such as $\sqrt{\sigma}/m_D$ would be non-zero and finite, the prediction of eqs. (3.1), (3.2) is that this ratio will diverge exponentially in β, and that it is the quantity $a^2\sigma\beta/am_D$ that has a finite limit. We will try to find some numerical evidence for this.

We remark that the glueball masses we will obtain in this section are consistent with those obtained in [8, 12, 13] but with much smaller errors. Our string tensions on the

JHEP01(2019)063

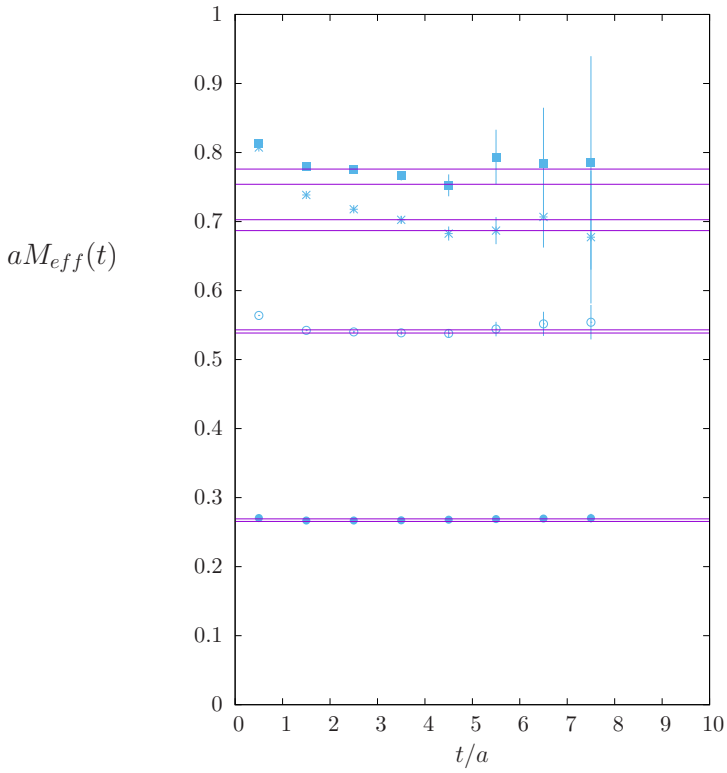

Figure 3. Effective masses for the 0^{--} ground state (•), the 0^{++} ground state (○), the 0^{--} first excited state (■) and the 2^{-+} ground state (⋆). All on a $50^2 36$ lattice at $\beta = 2.2$. Pairs of lines are our $\pm 1\sigma$ estimates of the corresponding masses.

other hand, while also being consistent with the values in [12, 13], are considerably less precise than the latter, because of the very different techniques employed. However our calculations are useful and complementary both because they are for closed flux tubes rather than the open flux tubes of [12, 13], and also, more importantly, because we are able to calculate the energies of excited flux tubes, as we will do in section 5.

4.1 Glueball masses

We will calculate the lightest few glueball masses at two couplings, $\beta = 2.2$ and $\beta = 2.3$, and on a range of volumes. This will allow us to check for both finite lattice spacing and finite volume corrections. But before doing so we need to assess how reliably we can calculate these masses from our correlation functions. To illustrate this we show in figure 3 the effective masses extracted from the correlators of our best variationally selected operators. This is taken on one of our larger lattices at $\beta = 2.2$. We see that the lightest 0^{--} and 0^{++} have unambiguous effective mass plateaux and excellent overlaps. The first excited 0^{--} has a reasonably convincing plateau and a good overlap. The 2^{-+} has a significantly worse overlap and hence a less convincing plateau. Other ground states, apart from the 2^{++} which is very similar to the 2^{-+}, are heavier and the plateaux are harder to identify, so we not use that data here. As stated earlier, our main focus in the paper will be on

JHEP01(2019)063

lattice	$aM_{0^{--},gs}$	$aM_{0^{--},ex1}$	$aM_{0^{++},gs}$
$68^2 36$	0.2670(13)	0.7709(38)	0.5376(29)
$50^2 36$	0.2676(21)	0.7728(38)	0.5401(35)
$42^2 36$	0.2670(23)	0.7662(70)	0.5295(61)
$34^2 36$	0.2671(27)	0.745(12)	0.5316(68)
$26^2 36$	0.2636(22)	0.705(17)	0.5040(65)
$22^2 36$	0.2624(30)	0.690(12)	0.4995(66)
$18^2 36$	0.2647(29)	0.690(16)	0.4544(51)
$14^2 36$	0.2816(40)	0.76(11)	0.3912(25)

Table 1. Masses of the lightest and first excited $J^{PC} = 0^{--}$ glueballs, and of the lightest 0^{++} glueball, on various spatial volumes at $\beta = 2.2$.

lattice	$aM_{0^{--},gs}$	$aM_{0^{--},ex1}$	$aM_{0^{++},gs}$
$60^2 60$	0.2111(22)	0.6118(68)	0.4289(38)
$54^2 60$	0.2102(22)	0.6244(53)	0.4247(42)
$36^2 48$	0.2059(24)	0.5954(82)	0.4168(47)
$30^2 48$	0.2107(28)	0.5740(83)	0.3972(50)
$24^2 32$	0.2138(38)	0.5492(88)	0.3924(40)

Table 2. Masses of the lightest and first excited $J^{PC} = 0^{--}$ glueballs, and of the lightest 0^{++} glueball, on various spatial volumes at $\beta = 2.3$.

the lightest 0^{--} and 0^{++} masses and on the mass of the first excited 0^{--}, all of which are reasonably well determined.

We also show in figure 3 the $\pm 1\sigma$ error bands on the mass estimates obtained from the correlators. These are purely statistical errors and we see, for example, that the estimate of the error is smaller for the 2^{-+} than for the excited 0^{--}. On the other hand it is clear that any systematic error associated with identifying the effective mass plateau is larger for the 2^{-+}. The caveat from this is that for heavier particles the quoted errors can be severely underestimated.

Our estimates of the masses of the lightest 0^{--} and 0^{++} and the first excited 0^{--} are listed in tables 1 and 2 for $\beta = 2.2$ and 2.3 respectively. We see that the mass gap has 0^{--} quantum numbers, just as expected. While the mass gap exhibits no obvious finite volume corrections, this is not the case for the 0^{++} and the excited 0^{--}. We plot the 0^{++} and excited 0^{--} masses in figures 4, 5 for $\beta = 2.2, 2.3$ respectively. We also show horizontal lines corresponding to once, twice and thrice the large-volume mass gap. We observe that at both values of β we have $M^{gs}_{0^{++}} = 2M^{gs}_{0^{--}}$ within our quite small errors, once the volume is large enough, roughly $lM_{0^{--}} \geq 9$. At $\beta = 2.3$ we also see that $M^{ex}_{0^{--}} = 3M^{gs}_{0^{--}}$ within errors on large volumes, although at $\beta = 2.2$ there is a slight undershoot, which is presumably due to the interactions arising from higher order lattice corrections which will be larger at smaller β.

JHEP01(2019)063

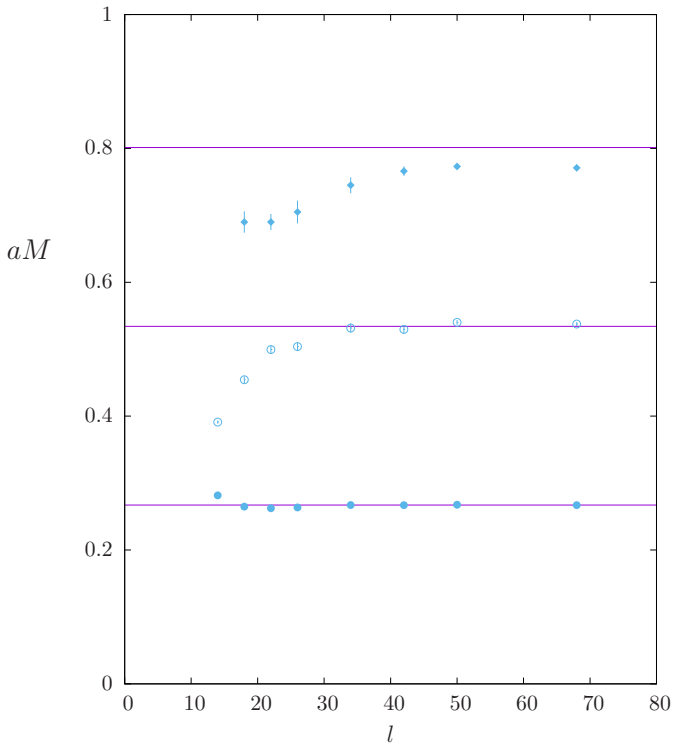

Figure 4. 0^{--} ground state (•), 0^{++} ground state (○) and 0^{--} first excited state (⧫) on spatial volumes $V = l^2$ at $\beta = 2.2$. Lines are once, twice, and thrice the large volume 0^{--} ground state mass.

Although we have seen in figure 3 that the $J = 2$ mass is less reliable (the systematic error is surely larger than the quoted statistical error) it is interesting to see what we find. In figure 6 we plot the $2^{\pm+}$ masses obtained on various volumes at $\beta = 2.3$. We also show the $2^{\pm-}$ masses; these are heavier and so a priori less reliable, but it so happens that their overlap is somewhat better and this partly compensates. The expectation in a free field theory is that the $2^{\pm+}$ will be composed of two 0^{--} particles, just like the 0^{++}, but that these will have non-zero relative momenta so as to project onto $J = 2$. As we decrease l the allowed momenta grow larger and so will the energy of the state (although lattice interactions will shift the actual momenta, e.g. by phase shifts) while as $l \to \infty$ we should see $M_{2^{\pm+}} \to 2M_{0^{--}}$ albeit slowly. For the $2^{\pm-}$ things are similar except that we need three 0^{--} particles so as to arrive at a net $C = -$, and so we expect $M_{2^{\pm-}} \to 3M_{0^{--}}$ as $l \to \infty$. Within the large errors, what we see in figure 6 roughly supports this scenario.

In summary what we see is consistent with the expectation that the 0^{++} ground state and the excited 0^{--} are composed of 2 and 3 non-interacting 0^{--} particles respectively up to lattice spacing corrections. As the volume decreases these 0^{--} particles will necessarily be closer and we would expect the effect of the lattice corrections on the energies of these states to be magnified, just as we observe. We shall indeed see below that the observed finite volume corrections do appear to disappear as we increase β.

JHEP01(2019)063

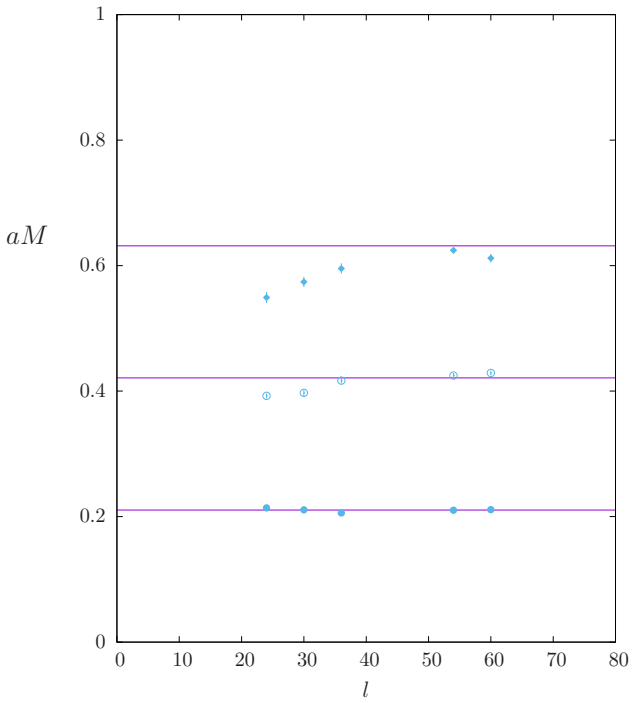

Figure 5. 0^{--} ground state (•), 0^{++} ground state (○) and 0^{--} first excited state (⧫) on spatial volumes $V = l^2$ at $\beta = 2.3$. Lines are once, twice and thrice the large volume 0^{--} ground state mass.

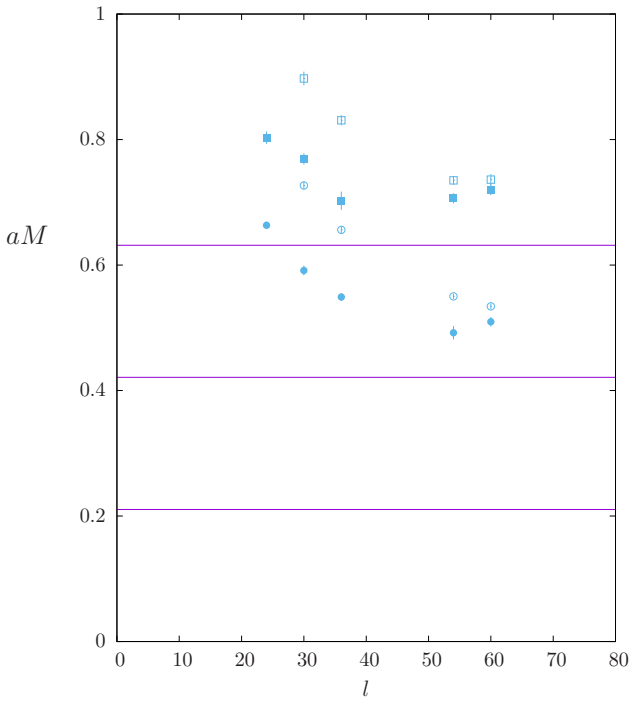

Figure 6. Ground state glueballs: 2^{++} (•), 2^{-+} (○) 2^{--} (■) and 2^{-+} (□) on spatial volumes $V = l^2$ at $\beta = 2.3$. Lines are once, twice and thrice the large volume 0^{--} ground state mass.

JHEP01(2019)063

l	$l_\perp$	$aE_{gs}^{P=+}$	$aE_{ex1}^{P=+}$	$aE_{ex2}^{P=+}$	$aE_{ex3}^{P=+}$	$aE_{ex4}^{P=+}$
9	75	0.1878(11)	0.4659(31)	0.5926(51)	0.6184(53)	
10	50	0.2190(12)	0.5090(44)	0.6647(42)	0.6984(60)	
14	64	0.3434(25)	0.6295(53)	0.760(11)	0.851(16)	
18	50,64,90	0.4617(17)	0.7492(30)	0.8555(50)	1.013(53)	
22	44,64	0.5785(25)	0.8565(50)	1.025(10)	1.157(7)	1.15(4)
26	42,64	0.6941(24)	0.9758(65)	1.123(9)	1.207(11)	1.20(4)
34	34	0.9130(47)	1.202(6)	1.319(13)	1.440(12)	1.51(4)
38	38	1.0310(36)	1.259(26)	1.393(15)	1.538(37)	1.59(3)
42	42	1.1472(57)	1.391(14)	1.492(14)	1.621(22)	1.62(4)
46	46	1.246(10)	1.497(15)	1.623(22)	1.727(25)	1.69(4)
50	50	1.356(9)	1.583(13)	1.695(22)	1.814(25)	1.85(5)
68	68	1.880(31)	2.11(6)	2.18(9)	2.20(12)	

Table 3. Energies of the lightest states of a flux tube of length l and positive parity P, winding around the x direction of the $l \times l_\perp$ spatial volume at $\beta = 2.2$.

4.2 String tension

On our periodic lattice we calculate the string tension σ from the energy of a confining flux tube that winds once around a spatial circle. This energy, $E_f(l)$, will depend on the spatial size l and, in the well studied case of SU(N) gauge theories [19–21], can be reliably related to σ by the expression in eq. (2.5), if l is not very small. The fact that eq. (2.5) encodes all the universal corrections of the effective string action describing a winding flux tube [15–18] suggests it will be equally applicable in the U(1) case, but clearly this needs to be checked. Accordingly we have performed calculations of $aE_f(l)$ for various l at $\beta = 2.2, 2.3$ as listed in tables 3, 4. The ground state of the flux tube has positive parity and appears in the tables as $E_{gs}^{P=+}$. Fitting this data with the expression in eq. (2.5), we find that we can get the following good fits over most of our range of l:

$$a^2\sigma = 0.027423(41)\,; \quad \frac{l}{a} \geq 14 \quad \frac{\chi^2}{n_{df}} = 0.68 \quad \beta = 2.2 \tag{4.2}$$

and

$$a^2\sigma = 0.020581(32)\,; \quad \frac{l}{a} \geq 17 \quad \frac{\chi^2}{n_{df}} = 0.81 \quad \beta = 2.3. \tag{4.3}$$

We can conveniently plot our results by scaling both the ground state energy E_f and the flux tube length l by the measured value of $\sqrt{\sigma}$ (which is essentially determined by large l) so that all quantities plotted become dimensionless: this allows us to place the $\beta = 2.2$ and $\beta = 2.3$ results on the same plot. This we do in figure 7 where we compare our values to the appropriately rescaled version of eq. (2.5). We see that the data is well described by eq. (2.5) and to emphasise this point we also plot the asymptotic $E_f = \sigma l$ fit, showing that the corrections to the linear piece that are encoded in eq. (2.5) are indeed important over a significant range of small l.

JHEP01(2019)063

l	$l_\perp$	$aE_{gs}^{P=+}$	$aE_{ex1}^{P=+}$	$aE_{ex2}^{P=+}$	$aE_{ex3}^{P=+}$	$aE_{gs}^{P=-}$	$aE_{ex1}^{P=-}$
17	74	0.3179(12)	0.5571(47)	0.677(14)	0.789(30)	0.673(7)	0.78(14)
21	74	0.4054(16)	0.6377(65)	0.773(12)	0.881(22)	0.742(7)	0.748(16)
26	74	0.5159(21)	0.7519(66)	0.894(27)	1.051(12)	0.811(13)	1.109(19)
30	50	0.5928(46)	0.842(10)	1.022(14)	1.088(17)	0.886(25)	1.132(18)
40	40	0.8085(34)	1.031(10)	1.069(54)	1.243(34)	1.083(18)	1.248(35)
44	44	0.8886(47)	1.090(19)	1.232(25)	1.331(12)	1.228(8)	1.354(11)
49	49	1.0009(54)	1.227(8)	1.306(11)	1.410(14)	1.368(13)	1.326(59)
53	53	1.0853(54)	1.291(30)	1.380(40)	1.501(70)	1.457(15)	1.515(21)
58	58	1.1957(86)	1.381(16)	1.488(21)	1.562(18)	1.561(17)	1.604(22)
79	79	1.628(27)	1.850(38)				

Table 4. Energies of the lightest states of a flux tube of length l winding around the x direction of the $l \times l_\perp$ spatial volume at $\beta = 2.3$, for both parities P.

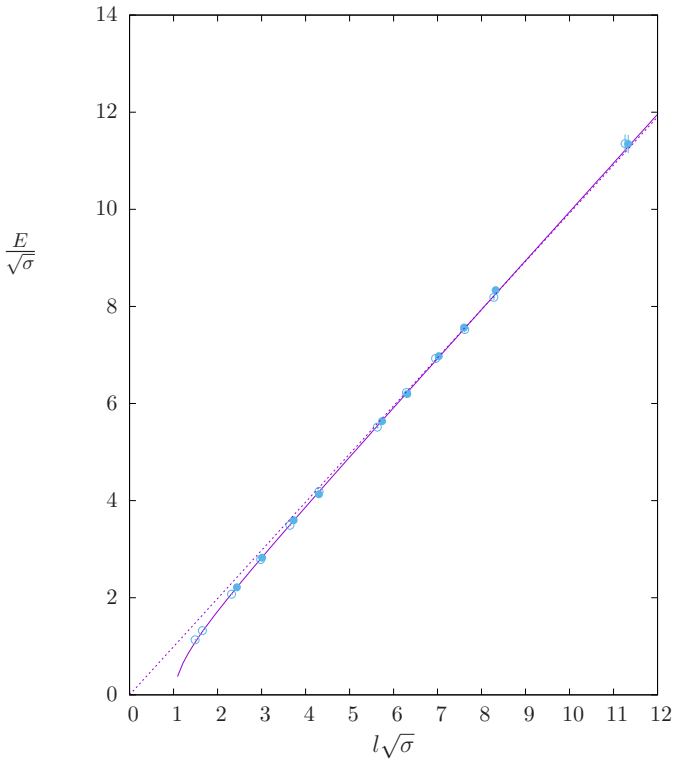

Figure 7. Ground state flux tube energy versus length l, at $\beta = 2.2$, $\circ$, and at $\beta = 2.3$, $\bullet$. Solid line is rescaled form of eq. (2.5) and dashed line is asymptotic $E = \sigma l$ piece.

Of course, just as for our glueballs, this analysis depends on the quality of our energy estimates. So in figure 8 we show the effective energy plots of the ground state flux tube for every second value of l. Clearly the effective energy plateaux are unambiguous (especially given the positivity constraint on $E_{\rm eff}$) except perhaps for $l = 68$, which has a large error

JHEP01(2019)063

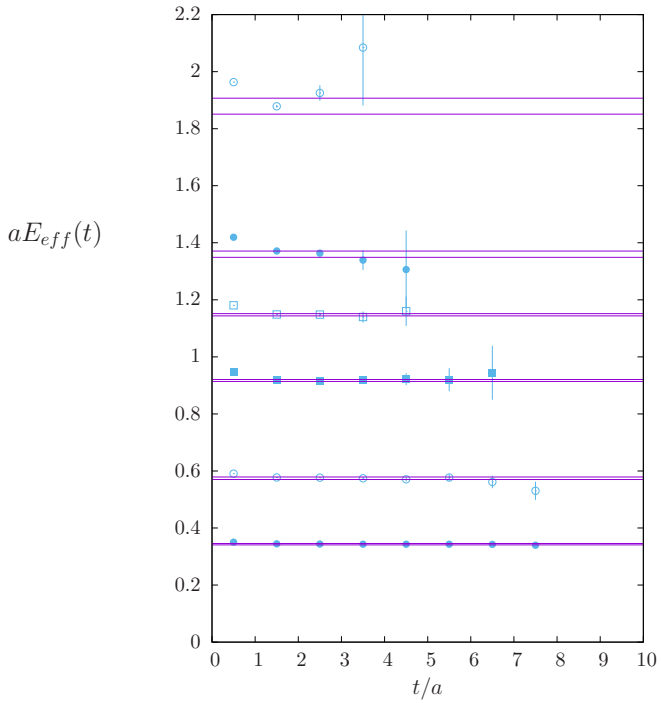

Figure 8. Effective energies of the ground states of winding flux tubes with lengths $l = 14, 22, 34, 42, 50, 68$ in increasing order. All at $\beta = 2.2$. Pairs of lines are our $\pm 1\sigma$ estimates of the corresponding energies.

and so does not play a significant role in our fits. In fact it is at small values of l that the corrections to the linear behaviour become important, and it is there that we have the best plateaux.

4.3 'Continuum' scaling

In addition to the above detailed calculations at $\beta = 2.2$ and $\beta = 2.3$ we have also performed some calculations over the much wider range $\beta \in [1.6, 2.8]$. The parameters and results of these calculations are listed in table 5. To keep the calculation manageable we have not made the lattices large enough, especially at large β, to be in the range of values of $lm_{0^{--}}$ where our calculations at $\beta = 2.2$ and $\beta = 2.3$ told us that finite volume corrections are negligible for all the tabulated quantities. So we can only be confident in the values we obtain for the string tension and the mass gap (except perhaps at $\beta = 2.8$) since these quantities are relatively insensitive to the volume, as we can see from tables 1 and 2. Nonetheless as a test of how the finite volume corrections vary with β it is interesting to look at our results for the masses of the ground state 0^{++} and the excited 0^{--} rescaled by the mass gap. This we do in figure 9, where we also show how the lattice size $lm_{0^{--}}$ varies with β for our lattices. What is interesting is that despite our decreasing volume (in physical units) the ratios rapidly approach their free field values as we increase β. This suggests that the corrections that we have seen to free field behaviour on small volumes are indeed due to the interactions arising from higher order lattice spacing corrections, as we

JHEP01(2019)063

β	*lattice*	$aM_{0^{--},gs}$	$aM_{0^{--},ex1}$	$aM_{0^{++},gs}$	$a\sqrt{\sigma}$
2.8	$62^2 110$	0.0598(40)	0.201(20)	0.1298(88)	0.07638(64)
2.7	$50^2 96$	0.0850(29)	0.249(15)	0.1691(52)	0.08562(106)
2.6	$44^2 96$	0.1054(32)	0.313(9)	0.2088(59)	0.09586(88)
2.5	$38^2 96$	0.1330(31)	0.368(13)	0.2588(86)	0.10953(84)
2.4	$38^2 64$	0.1610(28)	0.472(14)	0.3218(104)	0.12415(91)
2.3	$28^2 64$	0.2068(37)	0.544(15)	0.3940(83)	0.14473(43)
2.2	$22^2 48$	0.2692(27)	0.674(14)	0.4945(71)	0.16661(30)
2.1	$22^2 48$	0.3400(27)	0.877(13)	0.630(10)	0.19159(46)
2.0	$18^2 40$	0.4320(31)	1.062(21)	0.7884(50)	0.22250(39)
1.9	$18^2 40$	0.5514(26)	1.348(8)	0.978(11)	0.25877(28)
1.8	$18^2 40$	0.6996(21)		1.194(11)	0.3019(18)
1.7	$14^2 32$	0.8799(24)		1.407(19)	0.330(13)
1.6	$14^2 32$	1.0962(31)		1.635(41)	0.4078(16)

Table 5. Energies of the lightest glueball states and the string tension at various values of β on the lattices shown.

would expect. Of course, if we were to decrease the spatial size down towards $l \sim (1/T_c)$, then we would expect to see a change. However this is not a concern for the continuum limit since we have seen that $T_c/m_D \to \infty$ as $a \to 0$.

Returning to the quantities we are confident in, i.e. the string tension and the mass gap, we can ask if there is already evidence for the asymptotic $M_{0^{--}}/\sigma \propto \beta$ scaling implied by eqs. (3.1), (3.2). We plot this ratio in figure 10 and indeed we observe a very plausible linear growth with β except for the extreme point at $\beta = 2.8$. At this extreme value we begin to see an indication of a breakdown in the positivity of the flux loop correlator which may be due to critical slowing down. In any case the best linear fit shown in figure 10 is

$$\frac{am_{0^{--}}}{a^2\sigma} = -0.65(38) + 4.68(20)\beta \qquad 1.7 \geq \beta \geq 2.7, \quad \frac{\chi^2}{n_{df}} = 0.72. \tag{4.4}$$

This fit is obtained by maximising the interval in β over which we can obtain a good linear fit.The evidence for the non-zero constant piece in the fit is weak; indeed if restrict ourselves to the interval $2.0 \geq \beta \geq 2.7$ we obtain $am_{0^{--}}/a^2\sigma = 0.01(66) + 4.38(32)\beta$ for our best linear fit. In any case we note that the coefficient of β in these fits is remarkably close to the classical value $\pi^2/2 \simeq 4.93$ that we infer from eqs. (3.1), (3.2), (3.3).

It is also interesting to see whether the exponential behaviour of $am_{0^{--}} \equiv am_D$ in eq. (3.1) is reproduced in our calculations. We therefore plot in figure 11 the quantity $am_{0^{--}}/\sqrt{\beta}$ on a log-linear plot where an exponential appears as a straight line. Clearly the data displays such a linear behaviour to a good approximation and the fit shown is

$$\frac{am_{0^{--}}}{\sqrt{\beta}} = 59.4(1.1)\exp\{-2.633(10)\beta\} \qquad 1.7 \geq \beta \geq 2.8, \quad \frac{\chi^2}{n_{df}} = 1.34. \tag{4.5}$$

JHEP01(2019)063

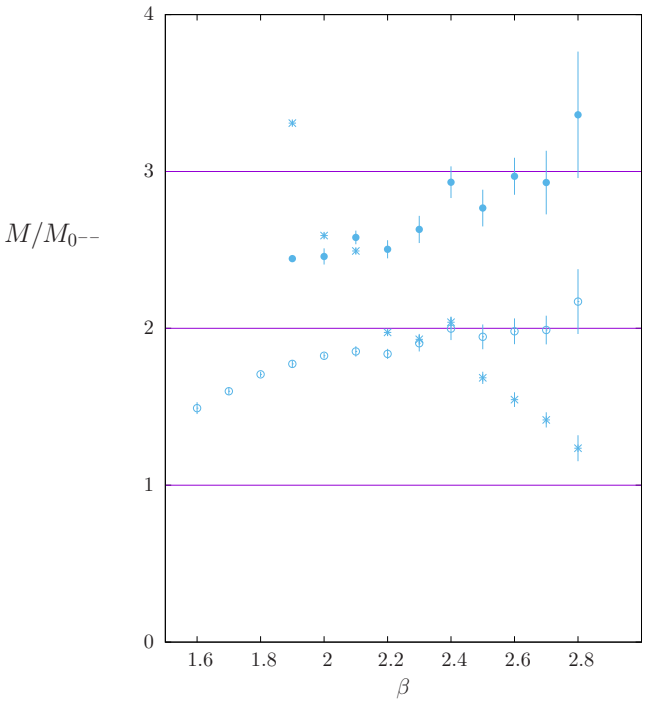

Figure 9. Masses of 0^{++} ground state ($\circ$) and 0^{--} first excited state ($\bullet$) in units of the mass of the 0^{--} ground state, versus β. Also $lM_{0^{--}}/3$ ($\star$), the rescaled spatial lattice size in units of the mass gap.

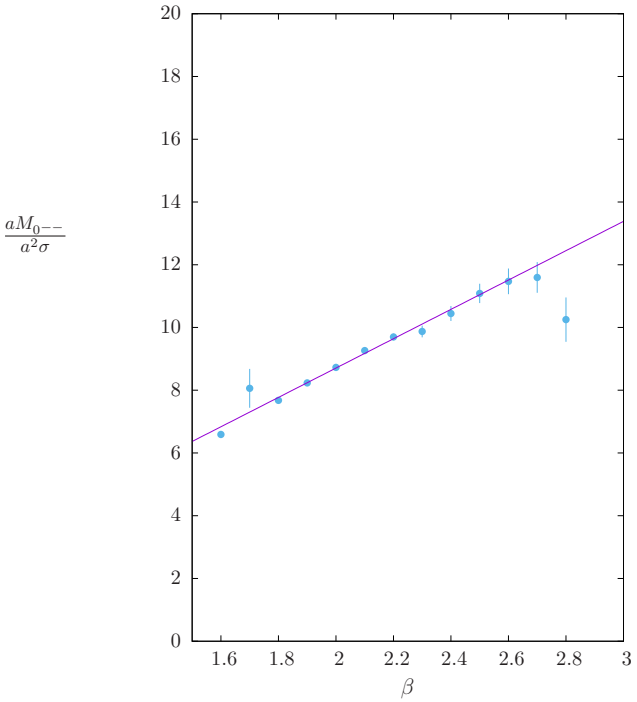

Figure 10. Mass of 0^{--} ground state divided by the string tension versus β.

JHEP01(2019)063

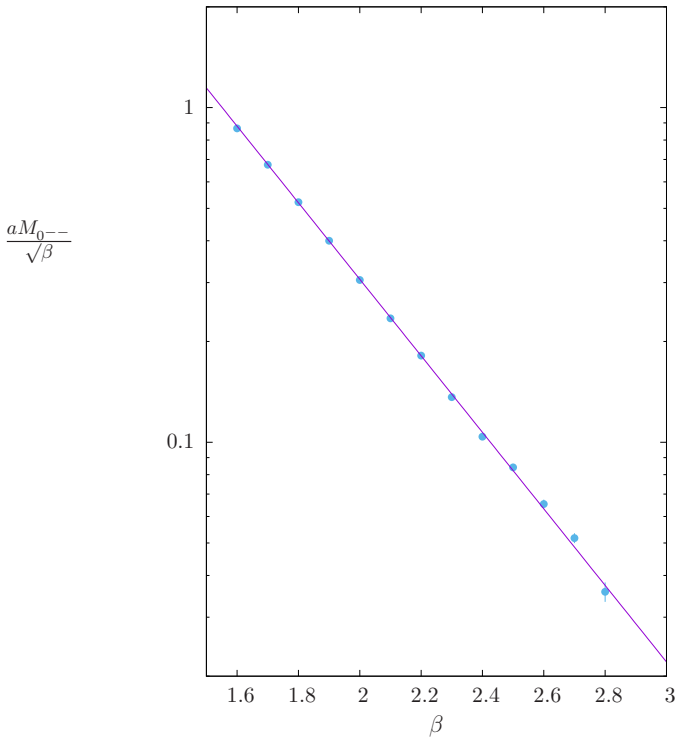

Figure 11. Mass of 0^{--} ground state rescaled by $\beta^{-1/2}$ versus β.

The theoretical classical value for the exponent is $0.2527\pi^2 \sim 2.494\beta$ which is remarkably close to the value in our above fit. The coefficient of the exponential is far from the classical value which is no surprise since it will be sensitive to quantum fluctuations. We repeat the exercise for the string tension, where we exclude the $\beta = 2.8$ value for the same reason as we did in eq. (4.4). In this case the fit is poor unless we also exclude several of the low β values. The data is displayed in figure 12 together with the fit

$$\sqrt{\beta}a^2\sigma = 11.5(6)\exp\{-2.561(22)\beta\} \qquad 2.1 \geq \beta \geq 2.7, \quad \frac{\chi^2}{n_{df}} = 1.93. \tag{4.6}$$

where once again we observe that the exponent is remarkably close to the the theoretical classical value. We note that, at least by eye, the fit appears to be reasonable over almost the whole range of β. This is however something of an illusion due to the errors being mostly too small to be visible on the plot. It may be puzzling that we can nonetheless have an acceptable fit to $am_{0^{--}}/\sqrt{\beta}$ over the range $1.7 \geq \beta \geq 2.7$, but this is due to the fact that the errors on that ratio are dominated by the errors from $am_{0^{--}}/\sqrt{\beta}$, which are much larger than those on $a^2\sigma$.

We conclude that our calculations show that both the mass gap and the string tension have a functional dependence on β that is very close to the theoretical expectation, even in our modest range of β.

JHEP01(2019)063

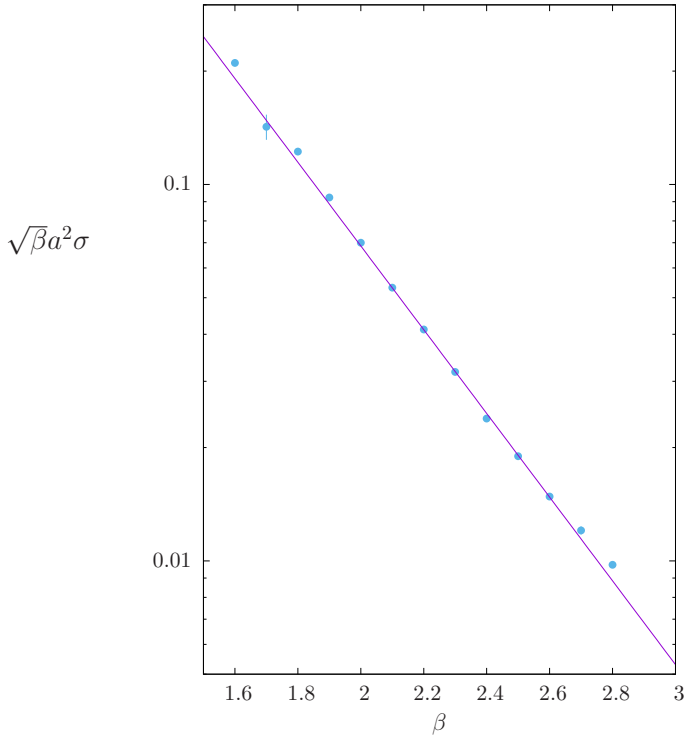

Figure 12. String tension rescaled by $\sqrt{\beta}$ versus β.

5 Flux tubes: spectrum and massive modes

In calculating the spectrum of the winding flux tube we obtain not just the energy of the ground state but also that of a number of excited states of the flux tube. In tables 3, 4 we present our energy estimates for the lightest 4/5 states with positive parity, $P = +$, at $\beta = 2.2$, and in addition the lightest two $P = -$ states at $\beta = 2.3$. We plot the $\beta = 2.2$ spectrum in figure 13 and the $\beta = 2.3$ one in figure 14. The curves on the plot are the predictions for the energies of the excited states as given by the string theory calculations that predict eq. (2.5) for the ground state [19–21]. These predictions actually work very well for the flux tube that carries fundamental flux in SU(N) gauge theories [19–21], the more so as N increases, and the theoretical reasons for this once mysterious success are now understood [35–37]. In the present case we see that there is no agreement except for the ground state. In fact what we see here is much like the spectrum of flux tubes in SU(N) that carry flux in the $k = 2A$ representation (the totally antisymmetric piece of $f \otimes f$) [19–21]. Just as in that case, we see a first excited state that has a nearly constant gap from the ground state until it begins to meet (and mix with) other excited states. This suggests that this state is not a 'stringy' excitation of the ground state, i.e. one which contains massless transverse excitations on the world sheet, but is simply the ground state with a massive excitation. If we plot the gap of this state from the ground state as a function of l, we see, in both figure 15 and figure 16, that the associated mass is consistent with that of the mass gap of the bulk theory. This is in contrast to the $k = 2A$ string

JHEP01(2019)063

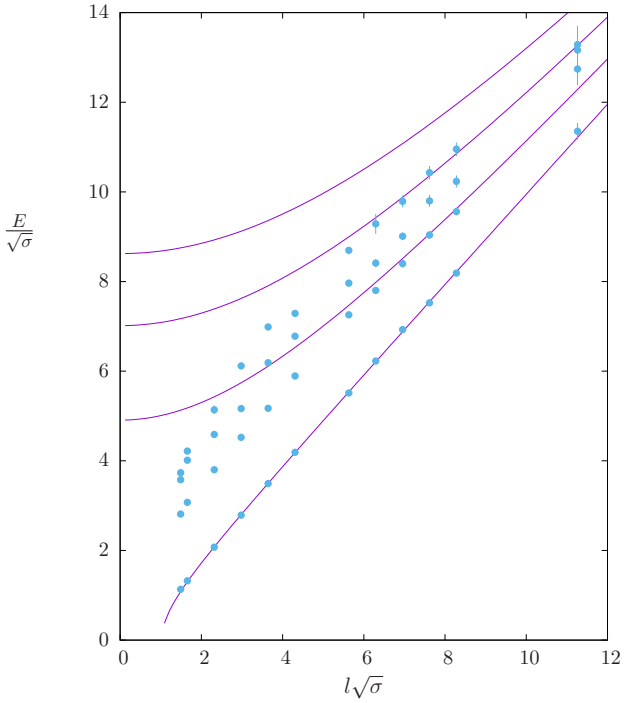

Figure 13. Positive parity flux tube spectrum versus length l, at $\beta = 2.2$. Lines are naive string theory predictions.

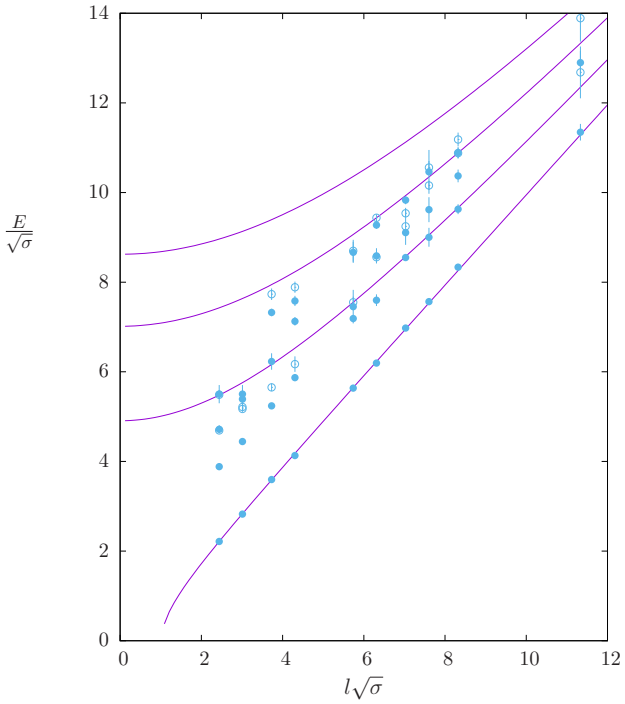

Figure 14. Flux tube spectrum versus length l, at $\beta = 2.3$. States with positive (•) and negative (○) parities. Lines are naive string theory predictions.

JHEP01(2019)063

in SU(N) in $D = 2 + 1$ [19–21] or the fundamental string in $D = 3 + 1$ SU(N) [38–40] where the mass of the excitation on the string world sheet is roughly half the mass gap. Given that the U(1) mass gap is just the screening mass, which one can label as a 'massive photon', one is tempted to conjecture that the world sheet mass in these SU(N) theories is that of a 'massive gluon'. The latter does not appear as an asymptotic state in the bulk theory because of colour confinement, but in the U(1) theory the photon has no charge and so is not affected by confinement.

Of course this interpretation is speculative. An operator involving a single winding loop will have a non-zero overlap onto a state consisting of a winding flux loop and a real massive photon (one will need some relative angular momentum to match the parities) and perhaps this is what we are seeing. (However our experience with SU(2), where there is also no large-N suppression, suggests that the overlap should be small.) We also note that the same mass appears in studies of the profile of the confining flux tube [12] at large distances from the axis of the tube, as one would expect since the asymptotic exponential decay of the profile should be governed by the mass gap. Finally we recall that the very accurate calculations in [13] for the ground state energy of flux tubes attached to static sources provided evidence for the contribution of a rigidity term in the world-sheet effective action, which involves a mass scale. Our ground state energies are not nearly accurate enough to test this idea for our closed flux tubes, so it would be very interesting to know whether such a rigidity term can reproduce the interesting behaviour of our first excited state.

This interference of a massive excitation on the world sheet depends very much on our calculation of the excited flux tube energy being reliable for the relevant range of l in figures 15 and 16. So once again it is useful to display the effective energy plots. This we do in figure 17 for $\beta = 2.2$ for all the values of l that play a significant role here. (At larger l the levels meet and appear to repel.) The identification of the effective energy plateaux appears reasonable, especially at the small to medium values of l, which are the most relevant.

6 Conclusions

After some preliminary calculations to localise the finite temperature deconfining phase transition, so as to be confident that we would be working in the low T confined phase, we focused on the calculation of the masses of 'glueballs' of various J^{PC} quantum numbers, and the energies of confining flux tubes that wind around a periodic spatial circle.

Our calculations of the lightest few glueball masses were entirely consistent with the theoretical expectation that the theory becomes a free field theory of massive particles as we approach the continuum limit. Our detailed finite volume studies of the glueball spectrum, at two modest values of $\beta = 2/ag^2$ showed that the lightest particle is indeed the $J^{PC} = 0^{--}$ 'massive photon' whose inverse mass $1/m_D$ provides the screening length of the monopole-instanton gas. We also saw that on large volumes the mass of the lightest 0^{++} is approximately $2m_D$ and that of the first excited 0^{--} is approximately $3m_D$. This is precisely what one expects if these states consist simply of the minimum number of the 'massive photons' with the minimum momenta consistent with those quantum numbers,

JHEP01(2019)063

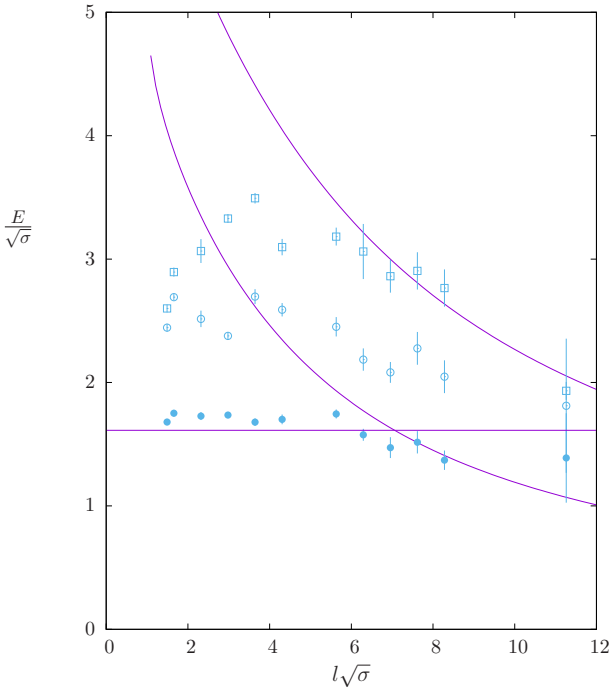

Figure 15. Difference between ground state energy and first (•), second (○) and third (□) excitations in figure 13. Horizontal line is the bulk mass gap. Falling lines are differences between ground and first/second excited string theory energies.

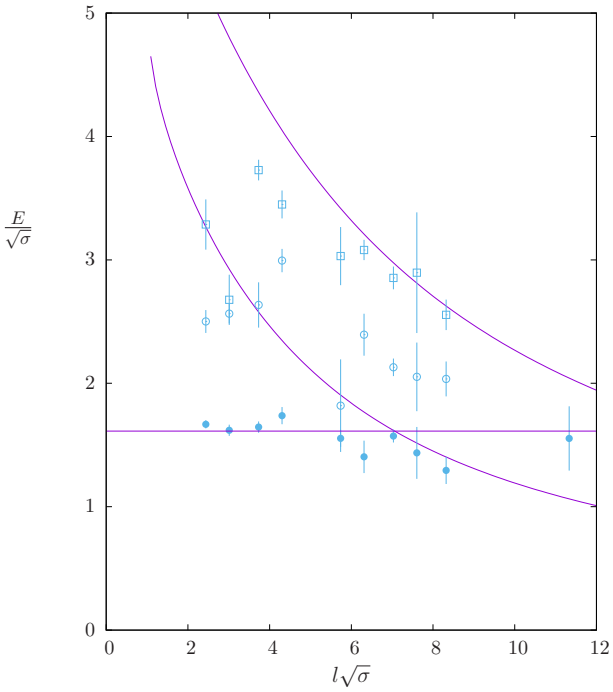

Figure 16. Difference between ground state energy and first (•), second (○) and third (□) $P = +$ excitations in figure 14. Horizontal line is the bulk mass gap. Falling lines are differences between ground and first/second excited string theory energies.

JHEP01(2019)063

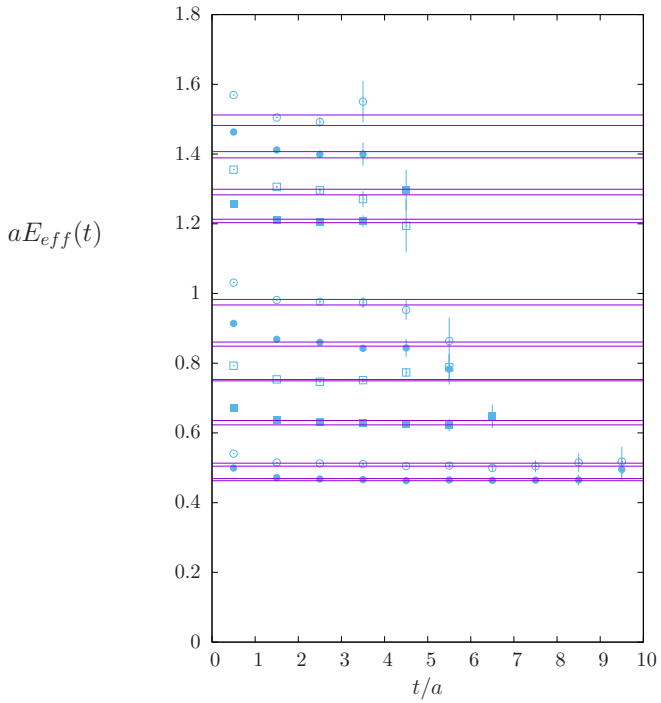

Figure 17. Effective energy of the first excited state of the winding flux tube with length $l = 9, 10, 14, 18, 22, 26, 34, 38, 42, 46$ in increasing order. At $\beta = 2.2$. Pairs of lines are our $\pm 1\sigma$ estimates of the corresponding energies.

and if there is no interaction energy, i.e. the theory is a free field theory. Our scan over a wider range of β appeared to confirm that the finite volume effects we saw were due to interactions mediated by lattice spacing corrections arising from the plaquette action we use. More importantly the scan provided a nice confirmation of the theoretically expected scaling behaviour $am_D/a^2\sigma \propto \beta$ as well as the expected exponential decay with β of both $am_D/\beta^{1/2}$ and $\beta^{1/2}a^2\sigma$.

From our calculations of the ground state energy $E_f(l)$ of a winding flux tube of length l, we obtained the string tension σ using a standard formula that encodes all the known universal corrections to the linear piece. This formula turns out to fit our energies very accurately down to small values of l, albeit not as small as in SU(N) gauge theories. We also calculated the energies of the lightest few excited states of the flux tube. These show little sign of a simple 'stringy' behaviour, and this is reminiscent of what one sees in SU(N) for flux tubes that carry a flux in a representation other than the fundamental — in particular the $k = 2A$ which is the antisymmetric piece of $f \otimes f$. Just as in the latter case the first excited state is consistent with being the ground state with a single massive excitation. The mass of this excitation is simply $\simeq m_D$. This differs from what we see in SU(N) in $D = 3 + 1$ where the mass of the world-sheet excitation is about one-half of the mass gap of the bulk theory. This may motivate the speculation that the latter mass may be that of a confined 'massive gluon' just like the non-confined 'massive photon' on the U(1) world sheet.

JHEP01(2019)063

Acknowledgments

AA has been financially supported by VI-SEEM and OPEN SESAME Horizon 2020 projects. MT acknowledges support by All Souls College and Oxford Theoretical Physics. The numerical computations were carried out on the computing cluster in Oxford Theoretical Physics.

JHEP01(2019)063

References

[1] A.M. Polyakov, *Compact gauge fields and the infrared catastrophe*, *Phys. Lett.* **B 59** (1975) 82 [INSPIRE].

[2] A.M. Polyakov, *Quark confinement and topology of gauge groups*, *Nucl. Phys.* **B 120** (1977) 429 [INSPIRE].

[3] A. Polyakov, *Gauge fields and strings*, Harwood Academic Publishers, Reading U.S.A. (1987).

[4] T. Banks, R. Myerson and J.B. Kogut, *Phase transitions in Abelian lattice gauge theories*, *Nucl. Phys.* **B 129** (1977) 493 [INSPIRE].

[5] M. Gopfert and G. Mack, *Proof of confinement of static quarks in three-dimensional* U(1) *lattice gauge theory for all values of the coupling constant*, *Commun. Math. Phys.* **82** (1981) 545 [INSPIRE].

[6] M. Karliner and G. Mack, *Mass gap and string tension in QED_3 comparison of theory with monte carlo simulation*, *Nucl. Phys.* **B 225** (1983) 371 [INSPIRE].

[7] K.R. Ito, *Upper and lower bound for the string tension in the three-dimensional lattice quantum electrodynamics*, *Nucl. Phys.* **B 205** (1982) 440 [*Erratum ibid.* **B 215** (1983) 136] [INSPIRE].

[8] M. Loan, M. Brunner, C. Sloggett and C. Hamer, *Path integral Monte Carlo approach to the* U(1) *lattice gauge theory in* $(2+1)$*-dimensions*, *Phys. Rev.* **D 68** (2003) 034504 [hep-lat/0209159] [INSPIRE].

[9] M.J. Teper, SU(N) *gauge theories in* $(2+1)$*-dimensions*, *Phys. Rev.* **D 59** (1999) 014512 [hep-lat/9804008] [INSPIRE].

[10] A. Athenodorou and M. Teper, SU(N) *gauge theories in* $2+1$ *dimensions: glueball spectra and k-string tensions*, *JHEP* **02** (2017) 015 [arXiv:1609.03873] [INSPIRE].

[11] R. Lau and M. Teper, SO(N) *gauge theories in* $2+1$ *dimensions: glueball spectra and confinement*, *JHEP* **10** (2017) 022 [arXiv:1701.06941] [INSPIRE].

[12] M. Caselle, M. Panero and D. Vadacchino, *Width of the flux tube in compact* U(1) *gauge theory in three dimensions*, *JHEP* **02** (2016) 180 [arXiv:1601.07455] [INSPIRE].

[13] M. Caselle, M. Panero, R. Pellegrini and D. Vadacchino, *A different kind of string*, *JHEP* **01** (2015) 105 [arXiv:1406.5127] [INSPIRE].

[14] M. Teper, *An improved method for lattice glueball calculations*, *Phys. Lett.* **B 183** (1987) 345 [INSPIRE].

[15] O. Aharony and Z. Komargodski, *The Effective Theory of Long Strings*, *JHEP* **05** (2013) 118 [arXiv:1302.6257] [INSPIRE].

[16] O. Aharony and E. Karzbrun, *On the effective action of confining strings*, *JHEP* **06** (2009) 012 [arXiv:0903.1927] [INSPIRE].

[17] S. Dubovsky, R. Flauger and V. Gorbenko, *Effective String Theory Revisited*, *JHEP* **09** (2012) 044 [arXiv:1203.1054] [INSPIRE].

[18] M. Lüscher and P. Weisz, *String excitation energies in* SU(N) *gauge theories beyond the free-string approximation*, *JHEP* **07** (2004) 014 [hep-th/0406205] [INSPIRE].

[19] A. Athenodorou and M. Teper, *Closed flux tubes in* $D = 2 + 1$ SU(N) *gauge theories: dynamics and effective string description*, *JHEP* **10** (2016) 093 [arXiv:1602.07634] [INSPIRE].

[20] A. Athenodorou and M. Teper, *Closed flux tubes in higher representations and their string description in* $D = 2 + 1$ SU(N) *gauge theories*, *JHEP* **06** (2013) 053 [arXiv:1303.5946] [INSPIRE].

[21] A. Athenodorou, B. Bringoltz and M. Teper, *Closed flux tubes and their string description in* $D = 2 + 1$ SU(N) *gauge theories*, *JHEP* **05** (2011) 042 [arXiv:1103.5854] [INSPIRE].

[22] E. Seiler, *Upper Bound on the Color Confining Potential*, *Phys. Rev.* **D 18** (1978) 482 [INSPIRE].

[23] T. Copeland, *Monopoles and Confinement in* U(1) *Lattice Gauge Theory*, Ph.D. Thesis, Oxford University, Oxford U.K. (1990).

[24] R. Wensley, *Monopoles And* U(1) *Lattice Gauge Theory*, Ph.D Thesis, University of Illinois, Chicago U.S.A. (1989), preprint ILL-TH-89-25.

[25] R.J. Wensley and J.D. Stack, *Monopoles and Confinement in Three-dimensions*, *Phys. Rev. Lett.* **63** (1989) 1764 [INSPIRE].

[26] P.A.M. Dirac, *Quantised singularities in the electromagnetic field*, *Proc. Roy. Soc. Lond.* **A 133** (1931) 60 [INSPIRE].

[27] T.A. DeGrand and D. Toussaint, *Topological Excitations and Monte Carlo Simulation of Abelian Gauge Theory*, *Phys. Rev.* **D 22** (1980) 2478 [INSPIRE].

[28] J. Villain, *Theory of one- and two-dimensional magnets with an easy magnetization plane. II. The planar, classical, two-dimensional magnet*, *J. Phys. France* **36** (1975) 581.

[29] Z. Schram and M. Teper, *Identifying monopoles on a lattice*, *Phys. Rev.* **D 48** (1993) 2881 [INSPIRE].

[30] B. Svetitsky and L.G. Yaffe, *Critical Behavior at Finite Temperature Confinement Transitions*, *Nucl. Phys.* **B 210** (1982) 423 [INSPIRE].

[31] J.M. Kosterlitz and D.J. Thouless, *Ordering, metastability and phase transitions in two-dimensional systems*, *J. Phys.* **C 6** (1973) 1181 [INSPIRE].

[32] O. Borisenko, V. Chelnokov, M. Gravina and A. Papa, *Deconfinement and universality in the* $3D$ U(1) *lattice gauge theory at finite temperature: study in the dual formulation*, *JHEP* **09** (2015) 062 [arXiv:1507.00833] [INSPIRE].

JHEP01(2019)063

[33] M.N. Chernodub, E.-M. Ilgenfritz and A. Schiller, *A Lattice study of $3-D$ compact QED at finite temperature*, *Phys. Rev.* **D 64** (2001) 054507 [hep-lat/0105021] [INSPIRE].

[34] P.D. Coddington, A.J.G. Hey, A.A. Middleton and J.S. Townsend, *The Deconfining Transition for Finite Temperature* U(1) *Lattice Gauge Theory in (2+1)-dimensions*, *Phys. Lett.* **B 175** (1986) 64 [INSPIRE].

[35] S. Dubovsky, R. Flauger and V. Gorbenko, *Flux Tube Spectra from Approximate Integrability at Low Energies*, *J. Exp. Theor. Phys.* **120** (2015) 399 [arXiv:1404.0037] [INSPIRE].

[36] S. Dubovsky, R. Flauger and V. Gorbenko, *Solving the Simplest Theory of Quantum Gravity*, *JHEP* **09** (2012) 133 [arXiv:1205.6805] [INSPIRE].

[37] S. Dubovsky and V. Gorbenko, *Towards a Theory of the QCD String*, *JHEP* **02** (2016) 022 [arXiv:1511.01908] [INSPIRE].

[38] S. Dubovsky, R. Flauger and V. Gorbenko, *Evidence from Lattice Data for a New Particle on the Worldsheet of the QCD Flux Tube*, *Phys. Rev. Lett.* **111** (2013) 062006 [arXiv:1301.2325] [INSPIRE].

[39] A. Athenodorou and M. Teper, *On the mass of the world-sheet 'axion' in* SU(N) *gauge theories in* $3+1$ *dimensions*, *Phys. Lett.* **B 771** (2017) 408 [arXiv:1702.03717] [INSPIRE].

[40] A. Athenodorou, B. Bringoltz and M. Teper, *Closed flux tubes and their string description in* $D=3+1$ SU(N) *gauge theories*, *JHEP* **02** (2011) 030 [arXiv:1007.4720] [INSPIRE].

JHEP01(2019)063